Interlevel electromagnetic response of systems of spherical quantum dots

Victor Bondarenko,[1,2,*] Miroslaw Załużny,[3] and Yang Zhao[1]
[1]*Department of Electrical and Computer Engineering, Wayne State University, Detroit, Michigan 48202, USA*
[2]*Department of Theoretical Physics, Institute of Physics, National Academy of Sciences of Ukraine, Kiev 03650, Ukraine*
[3]*Institute of Physics and Nanotechnology Center, M. Curie-Skłodowska University, 20-031 Lublin, Poland*
(Received 27 July 2004; revised manuscript received 27 September 2004; published 9 March 2005)

Interlevel electromagnetic response of individual spherical quantum dots (SQDs) as well as of two-dimensional (2D) rectangular lattice of spherical quantum dots is considered employing the self-consistent field approach in the quasistatic limit. It is established that the response can be considerably affected by the dynamic direct intradot and interdot electron-electron interaction. It is shown that the effects of these intradot and interdot interactions on the response can be analyzed separately. We show that correct description of the Coulomb coupling must take into account relevant umklapp processes. Fundamental importance of the problem of the electron self-interaction in quantum dot systems is established. The values are found which can be used for instant approximate estimation of the resonant dynamic screening (the depolarization shift) in *any* single SQD and 2D square lattice of SQDs. The effect of the size parameters of the systems, the SQD radius R and the lattice period d (and, in part, the three-dimensionality of the systems) on the depolarization shift is thoroughly investigated. Effect of polarization of incident radiation is investigated too. It is shown that the difference between the resonant photon energies for the normal and in-plane light polarization can be treated as independent of the static interdot interaction. Two-state and four-state electron systems are considered. Numerical calculations of the absorption spectra are performed for short period ($d/2R \leqslant 5$) lattices of GaAs spherical quantum dots in the $Al_{0.3}Ga_{0.7}As$ medium. It is established that the approximation of the point dipole-dipole interaction can be used for adequate representation of the dynamic interdot electron-electron interaction in the lattice. Also it is shown that the approach of the modified oscillator strength reproduces the absorption spectra of the considered systems with interacting modes of the collective excitation very well.

DOI: 10.1103/PhysRevB.71.115304 PACS number(s): 78.67.Hc, 73.21.La, 73.22.−f

I. INTRODUCTION

The electromagnetic response of quantum dots (QDs) due to interlevel transitions has been an attractive problem since QDs became objects for intensive fundamental research and application. One of the main points is how strongly the far-infrared (FIR) interlevel absorption spectra are affected by intradot and interdot electron-electron (e-e) interaction. A large number of theoretical and experimental works in this field have been done (see, e.g., Refs. 1 and 2). In most of the papers the authors assume that QDs have cylindrical symmetry with in-plane parabolic-like confining potentials.[1,3] A parabolic (harmonic) type of confining potential has a great advantage for analytical calculations. It was established that, when the confining potential of a many-electron system has parabolic shape, the e-e interaction does not affect the long-wavelength interlevel resonant frequency of the system.[4–6] This statement is applied to single harmonic quantum dots as well as to arrays of identical harmonic dots.[7] [More precisely the above statement is valid only for the optically active (Kohn) mode.] Consequently, the FIR absorption spectrum of the whole many-particle system agrees exactly with the spectrum of a single-particle system. Note that the approximation of the parabolic potential was shown to represent the potential usually experienced by an electron in large size QDs with a large amount of the electrons well. The situation is more complex and simultaneously more interesting in the case of a lattice of nonparabolic quantum dots with a few electrons per dot (or hole dots with different effective masses). The experimental results reported in Ref. 2 indicate that then the resonant photon energy is blueshifted against the corresponding interlevel spacing (renormalized by static Coulomb interaction) in individual dots. This shift is associated with the formation of the collective interlevel excitations due to the dynamic Coulomb force. In the literature the blueshift of the resonant photon energy induced by the dynamic direct Coulomb interaction is called the resonant screening or the depolarization effect (DE).

The subject of this paper is an investigation of the influence of the direct Coulomb interaction on the FIR absorption in spherical quantum dots (SQDs). Interlevel optical transitions in SQDs in the absence of the e-e interaction have been discussed theoretically by several groups.[8–10] The influence of the dynamic direct Coulomb interaction on the interlevel electromagnetic response of single SQDs (with the parabolic self-consistent confining potential) was considered, taking into account retardation effects, in Ref. 11. The main purpose of the present paper is to discuss the role of the intradot and interdot direct Coulomb interaction on the interlevel electromagnetic response of SQD systems. We consider the response of an individual SQD as well as two-dimensional rectangular lattice of spherical quantum dots (2DRLSQDs). In the later case different polarizations of the incident light are discussed. Our approach is based on the commonly used self-consistent field formalism[12–14] taking into account static and dynamic (direct) Coulomb interaction in the nonretarded (quasistatic) limit. Numerical calculations are performed for n-type $GaAs/Al_{0.3}Ga_{0.7}As$ quantum dots in which electrons are confined by a steplike hard-wall spherical potential. To

avoid considering mechanisms of loading electrons into the quantum dots we assume that each SQD contains a fixed number (N_{QD}) of electrons and k_BT is considerably smaller than the interlevel spacing. We concentrate on the cases when (i) the lowest level is occupied by one or two electrons ($N_{\mathrm{QD}}=1,2$) and (ii) two lowest levels are fully occupied ($N_{\mathrm{QD}}=8$). A special attention is paid to the problem of the electron self-interaction and coupling between interlevel collective modes. To our knowledge, this is the first time that the self-interaction problem is addressed in the investigation of the QD system response. We demonstrate the usefulness of the concept of the modified oscillator strength for description of the effects connected with intermode coupling. For comparison the interdot *e-e* interaction in the lattice is also considered within the approximation of the dipole-dipole interaction. We show that this approximation reproduces the exact result very well.

Since due to technological progress SQDs can now be manufactured[15,16] the problem of the interlevel transitions in such quantum dots is important for basic research as well as for applications (see also Ref. 9). Also, the effect of spherical symmetry is found to manifest itself in the collective excitations in other nanosystems.[17] In addition, growth of long-range ordered arrays of self-assembled quantum dots have been demonstrated[18] recently, with the quantum dots showing excellent optical properties.

The paper is organized as follows. Section II gives analytical development of the relationships used for numerical calculations. An outline of the density matrix approach to the response of the quantum dot systems is given in Sec. II A. Cases of a single SQD and 2DRLSQD are considered separately in Secs. II A 1 and II A 2, respectively. In Sec. II B the response of the two-state and four-state electron systems is analyzed in detail in Secs. II B 1 and II B 2, respectively. In addition, the response is considered within the modified oscillator strength approach, in Sec. II B 3, and within the approximation of dipole-dipole interaction, in Sec. II B 4. Section III presents numerical results and their detailed discussion for lattices with one electron per QD (Sec. III A) and structures with infinite (Sec. III B) and finite (Sec. III C) depths of the confining potential. The main conclusions are collected in Sec. IV. The Appendix explores the effect of static interdot interaction on the interlevel spacing in 2DRLSQDs.

II. THEORETICAL BACKGROUND

A rigorous approach to the problem of optical response of quantum dot systems is very complicated, particularly when we go beyond the two-level model. In general, it requires a self-consistent solution of the Maxwell equations with induced current density as a source term, which is related nonlocally to the field to be solved.[19] In this paper we employ a simpler formalism based on the density matrix approach in the quasistatic limit and the dipole approximation (see, e.g., Refs. 12 and 20). It has good justification when the wavelength of the incident radiation (λ) in the host medium is much larger than the dot radius (R) and (in the case of 2DRLSQDs) the interdot distance (d).

A. Density matrix approach to response of quantum dot systems

We investigate the electron interlevel electromagnetic response of the following systems of *three-dimensional* quantum dots: (i) single isolated SQDs and (ii) two-dimensional rectangular lattices containing N spherical quantum dots. In both cases we assume that the system is subjected to a linear-polarized (in the $\mathbf{e}_j$ direction) external electromagnetic field of the form $\mathbf{E}^{\mathrm{ext}}(t)=\mathbf{e}_j\tilde{E}_j(\omega)e^{-i\omega t}$ (the dipole approximation) which causes the interlevel electron transitions. We are interested in the multielectron QD systems. The Cartesian coordinate system (x_1,x_2,x_3), with the basis vectors, denoted by $\mathbf{e}_j$ $(j=1,2,3)$, is chosen so that the coordinate axes are directed along the symmetry axes of the system if any. In the case of the 2D rectangular lattice one coordinate axis is normal to the lattice plane, and the other axes are directed along the translation vectors $\mathbf{d}_1$ and $\mathbf{d}_2$ of the lattice, i.e., $\mathbf{e}_{1(2)}\|\mathbf{d}_{1(2)}$ and $\mathbf{e}_3\|(\mathbf{d}_1\times\mathbf{d}_2)$. In the following we present a general approach from first principles to calculate the interlevel electromagnetic response of a multilevel multielectron quantum system within the density matrix approximation.

It is convenient to describe the interlevel electromagnetic response of the system in terms of the (complex) tensor of the linear polarizability of the system $\overline{\boldsymbol{\alpha}}=\overline{\boldsymbol{\alpha}}'+i\overline{\boldsymbol{\alpha}}''$. This tensor is connected with the dipole moment induced in the system $[\mathbf{p}(t)=\mathbf{p}(\omega)e^{-i\omega t}]$ by the relation $p_j(\omega)=\overline{\alpha}_{jj}(\omega)\tilde{E}_j(\omega)$. In general, the tensor $\overline{\boldsymbol{\alpha}}$ is diagonal, i.e., $\overline{\alpha}_{ij}=\overline{\alpha}_{jj}\delta_{i,j}$. However, in the case of an isolated SQD it reduces to scalar $\overline{\alpha}_{ij}=\alpha\delta_{i,j}$. The power dissipated in the system $\mathcal{P}(\omega)[=\sum_j\mathcal{P}^{(j)}(\omega)]$ is associated with $\overline{\alpha}_{jj}$ by the relationship $\mathcal{P}^{(j)}(\omega)=(\omega/2)\overline{\alpha}''_{jj}|\tilde{E}_j|^2$. (Writing the above relation we have neglected the polaritonic effect.) Thus, spectral shape of the interlevel absorption of the system is controlled by $\overline{\alpha}''_{jj}(\omega)$. At this point it is interesting to note that while describing the experimental data on two-dimensional lattices of QDs it is convenient to treat the lattice as a pure two-dimensional effective sheet (see, e.g., Refs. 21 and 22) which is described by the 2D complex (effective) susceptibility tensor $\boldsymbol{\chi}^{\mathrm{2D}}$ (see, e.g., Refs. 21 and 23). This tensor is derived from the tensor $\overline{\boldsymbol{\alpha}}$ by the simple relationship $\boldsymbol{\chi}^{\mathrm{2D}}=\overline{\boldsymbol{\alpha}}/(\epsilon_0 S)$, where ϵ_0 is the free-space permittivity and $S=Nd_1d_2$ is the 2D area occupied by the lattice.

In the linear approximation the dipole moment induced in the system is associated with the density matrix $\rho(t)$ describing the system by $p_j(\omega)=-e\mathrm{Tr}[\rho^{(1,j)}(\omega)r_j]$. Consequently, the relationship for the polarizability takes the form

$$\overline{\alpha}_{jj}(\omega)=\frac{-e}{\tilde{E}_j(\omega)}\sum_{\nu,\nu'}\rho^{(1,j)}_{\nu\nu'}(\omega)(r_j)_{\nu'\nu}, \tag{1}$$

where $-e$ is the electron charge, $\mathbf{r}=(x_1,x_2,x_3)$, ν and ν' label the states of the electron system, and $\rho^{(1,j)}(\omega)$ is the first harmonic of the density matrix describing the system when the incident radiation is polarized in the $\mathbf{e}_j$ direction.

The equation governing the density matrix operator $\rho(t)$ is

$$\frac{\partial \rho^{(j)}_{\nu\nu'}(t)}{\partial t} = \frac{1}{i\hbar}[H_0 + V^{(j)}(t), \rho(t)]_{\nu\nu'} - \frac{[\rho^{(j)}(t) - \rho^{(0)}]_{\nu\nu'}}{\tau_{\nu\nu'}}. \tag{2}$$

Here H_0 is the Hamiltonian describing the electrons in the system in absence of the external field, $V^{(j)}(t)[=V^{(j)}(\omega)e^{-i\omega t}]$ is the perturbing potential, $\rho^{(0)}$ is the equilibrium value of the density matrix operator, and $\tau_{\nu\nu'}=\hbar/\Gamma_{\nu\nu'}$ is the scattering rate. The spatial dependence in Eq. (2) is omitted.

A general form of the first-harmonic solution of Eq. (2) is

$$\rho^{(1,j)}_{\nu\nu'}(\omega) = V^{(j)}_{\nu\nu'}(\omega)\frac{\Delta\rho^{(0)}_{\nu\nu'}}{E_{\nu\nu'} - \hbar\omega - i\Gamma_{\nu\nu'}}, \tag{3}$$

which is utilized in Eq. (1). Here $E_{\nu\nu'}=E_\nu - E_{\nu'}$ with $E_\nu = \langle\nu|H_0|\nu\rangle$ and $\Delta\rho^{(0)}_{\nu\nu'}=\rho^{(0)}_{\nu\nu}-\rho^{(0)}_{\nu'\nu'}$. It is important to emphasize that $\rho^{(0)}_{\nu\nu}(\equiv n_\nu)$ represents the number of electrons at state ν in the *whole* electron system under consideration. Then $\Delta\rho^{(0)}_{\nu\nu'}=n_{\nu\nu'}=n_\nu - n_{\nu'}$ represents the number of the electrons in the whole electron system involved in the $\nu\rightarrow\nu'$ transitions, and $\Gamma_{\nu\nu'}$ is the broadening parameter associated with these transitions. $V^{(j)}_{\nu\nu'}\equiv\langle\nu|V^{(j)}(\mathbf{r},\omega)|\nu'\rangle$ is the matrix element of the perturbing potential $V^{(j)}(\mathbf{r},\omega)$ which in the self-consistent field approach is presented by the following relationship:

$$V^{(j)}(\mathbf{r},\omega) = V^{(j)\mathrm{ext}}(\mathbf{r},\omega) + \frac{e^2}{4\pi\epsilon\epsilon_0}\int d\mathbf{r}'\frac{1}{|\mathbf{r}-\mathbf{r}'|}\sum_{\nu\nu'}\rho^{(1,j)}_{\nu\nu'}(\omega) \times\Psi^*_{\nu'}(\mathbf{r}')\Psi_\nu(\mathbf{r}'), \tag{4}$$

where Ψ_ν is the eigenfunction of state ν. Here the first term $V^{(j)\mathrm{ext}}(\mathbf{r},\omega)=e\tilde{E}_j(\omega)r_j$ is the external perturbing potential and the second term, shortly $V^{(j)\mathrm{ind}}(\omega)$, stands for the correction induced due to the dynamic *e-e* interaction. ϵ is the background dielectric constant of the medium. In the systems considered in this paper, the difference between the dielectric constants of the well and barrier materials is rather small. Thus, so-called dielectric effects can be neglected in the first approximation.[10]

To self-consistently solve Eqs. (3) and (4) we exploit the approach developed in our previous paper[20] on quantum well systems. A general form of the solution $\varrho^{(1,j)}_{\nu\nu'}(\omega)$ for the density matrix is obtained from the set of equations

$$\varrho^{(1,j)}_{\nu\nu'}(\omega) = \frac{V^{(j)\mathrm{ext}}_{\nu\nu'}n_{\nu\nu'}}{E_{\nu\nu'} - \hbar\omega - i\Gamma_{\nu\nu'}} + \frac{\sum_{\sigma,\sigma'}\mathcal{L}^{(j)}(\nu,\nu';\sigma,\sigma')\varrho^{(1,j)}_{\sigma\sigma'}(\omega)\mathcal{N}_{\nu\nu'}}{E_{\nu\nu'} - \hbar\omega - i\Gamma_{\nu\nu'}}, \tag{5}$$

where the first term on the right-hand side stands for the one-electron solution (which neglects the dynamic *e-e* interaction), while the second term represents the dynamic *e-e* interaction in the many-electron systems by means of $\mathcal{L}^{(j)}(\nu,\nu';\sigma,\sigma')$. The pairs $\nu\rightarrow\nu'$, $\sigma\rightarrow\sigma'$ cover all the interstate transitions in the system under consideration. The quantity $\mathcal{N}_{\nu\nu'}$ is related to $n_{\nu\nu'}$. For the quantum wells $\mathcal{N}_{\nu\nu'}=n_{\nu\nu'}$. As our present investigation shows the relation between $\mathcal{N}_{\nu\nu'}$ and $n_{\nu\nu'}$ is more complicated for QD systems where the electron self-interaction cannot be neglected. Due to this $\mathcal{L}^{(j)}(\nu,\nu';\sigma,\sigma')$ and $\mathcal{N}_{\nu\nu'}$ are specific to each many-electron system. In the following we apply the above approach to a single isolated QD as well as to 2D lattices of QDs.

Finally we would like to briefly consider within the above formalism the systems with the parabolic (harmonic) confining potential, which are known to obey the generalized Kohn's theorem:[4,24] the *e-e* interaction does not affect the FIR response of such systems. As the parabolic confining potential is the only one which allows separation of the center-of-mass (c.m.) variables and relative variables describing any kind of the *e-e* interaction of the system (see Ref. 24), this let us to separate the equation which governs $\rho_{\mathrm{c.m.}}(t)$ depending only on the (c.m.) variables from Eq. (2). It is $\rho_{\mathrm{c.m.}}(t)$ that determines $\mathbf{p}(t)$ which, thus, is not affected by the *e-e* interaction.

1. An isolated spherical quantum dot

First we consider optical transitions between bound levels in a *single isolated* SQD. The confining potential is assumed to be spherical steplike hard wall potential.

For brevity, in further discussions, an eigenstate of the one-band effective mass Hamiltonian H_0 in the single SQD will be denoted by composite quantum number $\mathbf{a}=(n,l,m)$, with $m=0,\pm1,\ldots,\pm l$, where n, l, and m are the main, azimuth, and the magnetic quantum numbers, respectively. (The spin quantum number is omitted for simplicity. It is conserved during the interlevel transitions.) The eigenenergy of H_0 will be denoted by $E_{\mathbf{a}}=E_{n,l}$. Due to the spherical symmetry of the system, the level with eigenenergy $E_{n,l}$ is $(2l+1)$-fold degenerate with respect to the angular momentum projection. In addition to the term "state of SQD" we shall use the term "energy level (shell) of SQD" to name all the states which share the same $E_{n,l}$.

The eigenfunction $\Psi_{\mathbf{a}}$ of H_0 is written in the form

$$\Psi_{n,l,m}(\mathbf{r}) = R_{n,l}(r)Y_{l,m}(\theta,\varphi), \tag{6}$$

where r is the distance from the SQD center and θ and φ are the angles in the spherical coordinates. The radial part of the wave function $R_{n,l}(r)=F_{n,l}(r)/r$ satisfies the equation

$$\left[-\frac{\hbar^2}{2}\frac{\partial}{\partial r}\frac{1}{m^*(r)}\frac{\partial}{\partial r} + V_{\mathrm{sc}}(r) + \frac{\hbar^2 l(l+1)}{2m^*(r)r^2}\right]F_{n,l}(r) = E_{n,l}F_{n,l}(r), \tag{7}$$

where $m^*(r)$ is the spatially dependent effective mass of the electron and $V_{\mathrm{sc}}(r)$ is self-consistent confining potential.

Note that the Hartree approximation is used here. Thus, $V_{\mathrm{sc}}(r)$ includes only the direct Coulomb interaction, while the exchange-correlation interaction is omitted. This approximation seems to have good justification for quantum dots with rather many electrons (see, e.g., Refs. 25 and 26). We expect that including the exchange-correlation interaction

can reduce the effect of the direct Coulomb interaction only quantitatively and does not affect the general (qualitative) conclusions of the paper. The effect of positive charges is not considered either. Although, in general, this effect reduces the effect of the static intradot *e-e* interaction, it depends on the distribution of the donors (inside and/or outside the SQD) and makes the calculations specific for each distribution. In our calculations we assume for simplicity that this interaction does not violate the spherical symmetry of the confining potential and can be neglected in the first approximation.

Equation (7) will be solved numerically following the approach developed in Refs. 27 and 26. Without the loss of generality we can assume that the electric field $\mathbf{E}^{\text{ext}}$ is directed along the $x_3(=z)$ direction and omit the polarization index. The matrix element of $z=r\cos\theta$ can be rewritten [employing Eq. (6)] in the form

$$z_{\mathbf{a},\mathbf{a}'} = \delta_{l\pm1,l'}\delta_{m,m'}Y^{l\pm1,|m|}_{l,|m|}R^{n',l\pm1}_{n,l}, \tag{8}$$

where $Y^{l',m'}_{l,m} = \int_0^{2\pi}d\varphi\int_0^{\pi}d\theta\sin\theta\cos\theta Y^*_{l',m'}(\theta,\varphi)Y_{l,m}(\theta,\varphi)$ and $R^{n',l'}_{n,l} = \int dr r^3 R^*_{n',l'}(r)R_{n,l}(r)$.

From Eq. (3) we obtain the matrix elements $\rho^{(1)}_{\mathbf{a},\mathbf{a}'}(\omega)$ of the density matrix by setting $\nu=\mathbf{a}$ and $\nu=\mathbf{a}'$. Then $E_{\mathbf{a},\mathbf{a}'}=E_{\mathbf{a}}-E_{\mathbf{a}'}$ is the interlevel spacing renormalized by the static intradot *e-e* interaction (see, e.g., Fig. 1 in Ref. 26). $\Delta\rho^{(0)}_{\mathbf{a},\mathbf{a}'}\equiv n_{\mathbf{a},\mathbf{a}'}=n_{\mathbf{a}}-n_{\mathbf{a}'}$, with $n_{\mathbf{a}}$ stands for the number of electrons at state $\mathbf{a}$ per dot, represents the number of electrons in the QD involved in the $\mathbf{a}\to\mathbf{a}'$ transitions. $V_{\mathbf{a},\mathbf{a}'}\equiv\langle\mathbf{a}|V(\mathbf{r},\omega)|\mathbf{a}'\rangle$ is the matrix element of the perturbing potential $V(\mathbf{r},\omega)$ [see Eq. (4)]. Now the second term in Eq. (4) represents the potential associated with intradot dynamic Coulomb interaction of electrons in the SQD.

Attention must be paid to the fact that in an individual QD (i) $V(\mathbf{r},\omega)$ in Eq. (4) is the self-consistent effective potential *existing* in the QD, that is, the potential which is created by all the electrons in the dot, (ii) the matrix element $V_{\mathbf{a},\mathbf{a}'}$ is calculated for the self-consistent effective potential which is *experienced* by an electron in the dot, which means that the potential of that electron must be excluded in $V_{\mathbf{a},\mathbf{a}'}$, and (iii) there are only a few electrons ($\leqslant 8$) in the dot. Thus, physically the second term in Eq. (4) should result in zero when $V_{\mathbf{a},\mathbf{a}'}$ is calculated for only one electron in the dot. However, this term (i.e., $V^{\text{ind}}_{\mathbf{a},\mathbf{a}'}$) in $V_{\mathbf{a},\mathbf{a}'}$ is equal to zero only when there is no electron in the dot, and it takes a nonzero value in the presence of any number, even one, of electrons in the dot.

For one electron in the dot $V^{\text{ind}}_{\mathbf{a},\mathbf{a}'}$ is the potential of the dynamic self-interaction of the electron with itself. This self-interaction contribution must be excluded from the effective potential. Keeping this contribution within the effective potential leads to considerable overestimation of the latter one. For instance, in the case of two electrons per single QD the effective induced potential would be twice as much as it is really. Note that there is no problem of this kind for quantum wells and wires, since there are plenty of electrons in the occupied subbands of those structures, and the relative contribution of the self-interaction to the effective potential is negligibly small.

Using Eq. (4) and taking into account the fact that due to the spherical symmetry of the potential $V_{\text{sc}}(r)$ only the optical transitions with $E_{\mathbf{a},\mathbf{a}'}\neq 0$ are allowed, we get that $\rho^{(1)}_{\mathbf{a},\mathbf{a}'}(\omega)$ is defined by Eq. (5) if we take $\nu=\mathbf{a}$, $\nu'=\mathbf{a}'$, $\sigma=\mathbf{b}$, $\sigma'=\mathbf{b}'$, and $\varrho^{(1,j)}_{\nu\nu'}(\omega)=\rho^{(1)}_{\mathbf{a},\mathbf{a}'}(\omega)$, $\mathcal{L}^{(j)}(\nu,\nu';\sigma,\sigma')=L^{(j)}(\mathbf{a},\mathbf{a}';\mathbf{b},\mathbf{b}')$, and $\mathcal{N}_{\nu\nu'}=n_{\mathbf{a},\mathbf{a}'}-\delta_{\mathbf{a},\mathbf{b}}\delta_{\mathbf{a}',\mathbf{b}'}$. We have introduced $\delta_{\mathbf{a},\mathbf{b}}\delta_{\mathbf{a}',\mathbf{b}'}$ into $\mathcal{N}_{\nu\nu'}$ to exclude the self-interaction. Here

$$L(\mathbf{a},\mathbf{a}';\mathbf{b},\mathbf{b}') = \frac{e^2}{4\pi\epsilon\epsilon_0}\int d\mathbf{r}\int d\mathbf{r}'\Psi^*_{\mathbf{a}}(\mathbf{r}) \times\Psi_{\mathbf{a}'}(\mathbf{r})\frac{1}{|\mathbf{r}-\mathbf{r}'|}\Psi^*_{\mathbf{b}'}(\mathbf{r}')\Psi_{\mathbf{b}}(\mathbf{r}'). \tag{9}$$

Note that the nondiagonal elements appear as a result of the coupling between different $\mathbf{a}\to\mathbf{a}'$ and $\mathbf{b}\to\mathbf{b}'$ transitions (modes).

For further calculations it is convenient to exploit, as in Ref. 5, the 2D Fourier expansion of $1/|\mathbf{r}-\mathbf{r}'|$

$$\frac{1}{|\mathbf{r}-\mathbf{r}'|} = \frac{1}{2\pi}\int d\mathbf{Q}_{\parallel}\frac{1}{Q_{\parallel}}e^{-i\mathbf{Q}_{\parallel}(\mathbf{r}_{\parallel}-\mathbf{r}'_{\parallel})}e^{-Q_{\parallel}|x_3-x'_3|}, \tag{10}$$

where two 2D vectors in the x_1-x_2 plane $\mathbf{r}_{\parallel}=(x_1,x_2)$ and $\mathbf{Q}_{\parallel}=(Q_1,Q_2)$ are introduced. Then the expression for $L(\mathbf{a},\mathbf{a}';\mathbf{b},\mathbf{b}')$ becomes

$$L(\mathbf{a},\mathbf{a}';\mathbf{b},\mathbf{b}') = \frac{e^2}{8\pi^2\epsilon\epsilon_0}\int d\mathbf{Q}_{\parallel}\frac{1}{Q_{\parallel}}\int dx_3dx'_3 \times e^{-Q_{\parallel}|x_3-x'_3|}A^-_{\mathbf{a},\mathbf{a}'}(\mathbf{Q}_{\parallel},x_3)A^+_{\mathbf{b}',\mathbf{b}}(\mathbf{Q}_{\parallel},x'_3), \tag{11}$$

where

$$A^{\pm}_{\mathbf{c},\mathbf{c}'}(\mathbf{Q}_{\parallel},x_3) = \int d\mathbf{r}_{\parallel}\Psi^*_{\mathbf{c}}(\mathbf{r}_{\parallel},x_3)e^{\pm i\mathbf{Q}_{\parallel}\mathbf{r}_{\parallel}}\Psi_{\mathbf{c}'}(\mathbf{r}_{\parallel},x_3). \tag{12}$$

It should be emphasized that the above approach can be used for other shapes of single QDs and Eq. (12) takes care of the shape.

Note that Eq. (11) does not impose any restrictions on the interlevel transitions of electrons in individual QDs. Applied to the spherical QDs, it is easy to see that $L(\mathbf{c},\mathbf{c}';\mathbf{c},\mathbf{c}')>0$ and $L(\mathbf{a},\mathbf{a}';\mathbf{b},\mathbf{b}')<0$ if $\mathbf{a}\neq\mathbf{b}$ and/or $\mathbf{a}'\neq\mathbf{b}'$.

Analysis of Eq. (5) for $\rho^{(1)}_{\mathbf{a},\mathbf{a}'}(\omega)$ (see also Sec. II B) shows that the strength of the depolarization effect in the single SQD is controlled by the product

$$\overline{L}_{\mathbf{a},\mathbf{a}';\mathbf{b},\mathbf{b}'} = L(\mathbf{a},\mathbf{a}';\mathbf{b},\mathbf{b}')(\sqrt{n_{\mathbf{a},\mathbf{a}'}n_{\mathbf{b},\mathbf{b}'}}-\delta_{\mathbf{a},\mathbf{b}}\delta_{\mathbf{a}',\mathbf{b}'}). \tag{13}$$

For example [see Eq. (31)], in the two-level approximation the resonant energy associated with the transitions between states $\mathbf{c}$ and $\mathbf{c}'$ is given by

$$\hbar\omega_{\text{res}} = E_{\mathbf{c},\mathbf{c}'}\sqrt{1-2\overline{L}_{\mathbf{c},\mathbf{c}';\mathbf{c},\mathbf{c}'}/E_{\mathbf{c},\mathbf{c}'}}. \tag{14}$$

It is important to emphasize that the factor $L(\mathbf{c},\mathbf{c}';\mathbf{c},\mathbf{c}')n_{\mathbf{c},\mathbf{c}'}$ (in contrast with $\overline{L}_{\mathbf{c},\mathbf{c}';\mathbf{c},\mathbf{c}'}$) represents the interaction energy with the self-interaction included, and the value of $L(\mathbf{c},\mathbf{c}';\mathbf{c},\mathbf{c}')$ itself is the energy caused by the self-

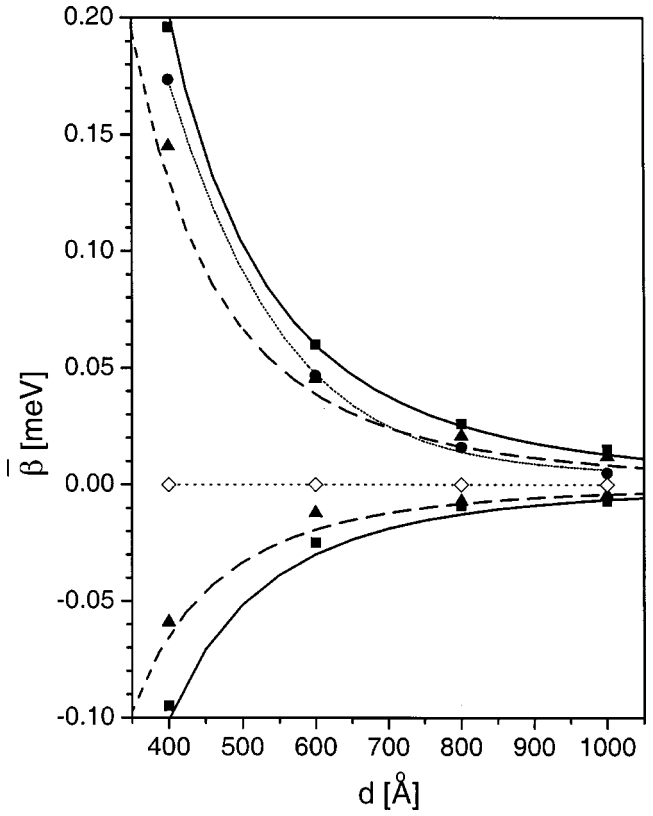

FIG. 1. Dependence of the DE shift associated with the interdot dynamic *e-e* interaction in a square lattice of SQDs upon the lattice period calculated within different approximations. One electron is per QD. $R=95$ Å. Square symbols represent SQDs with finite potential barrier. Triangular symbols represent infinite deep SQDs (the Bessel wave functions). The lines stand for the DDA, with the dipole matrix element being of the finite (solid lines) or infinite deep (dash lines) SQD. Positive (negative) values represent the normal (in-plane) polarization of the incident radiation. The zero level is also labelled by symbols in order to emphasize that the "zero" is also calculated (it is the self-interaction value). For comparison the change of the interlevel spacing because of the static interdot *e-e* interaction is presented by the dot line with circle symbols (see Fig. 8).

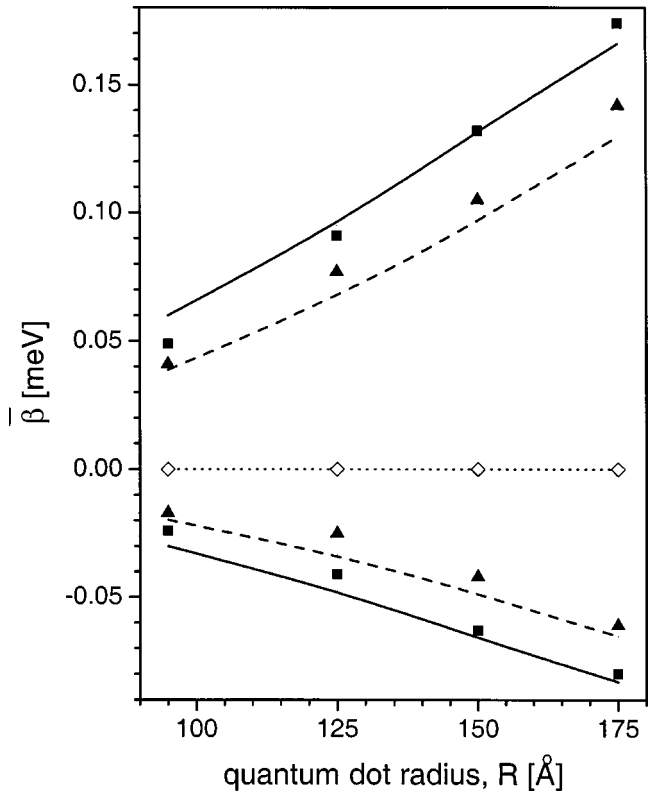

FIG. 2. Dependence of the DE shift caused by the interdot dynamic *e-e* interaction in a square lattice of SQDs upon the SQD radius calculated within different approximations. One electron is per QD. $d=600$ Å. The legend is the same as in Fig. 1.

interaction of one electron with itself in a single QD. Note that it is $L(\mathbf{c},\mathbf{c}';\mathbf{c},\mathbf{c}')$ that serves as the "calculated zero" in Figs. 1–3.

For further discussion it is useful to present $\overline{L}_{\mathbf{a},\mathbf{a}';\mathbf{b},\mathbf{b}'}$ for the SQD in the form

$$\overline{L}_{\mathbf{a},\mathbf{a}';\mathbf{b},\mathbf{b}'}=\frac{e^2}{\epsilon\epsilon_0 R}\tilde{L}_{\mathbf{a},\mathbf{a}';\mathbf{b},\mathbf{b}'}, \tag{15}$$

where $\tilde{L}_{\mathbf{a},\mathbf{a}';\mathbf{b},\mathbf{b}'}$ is a dimensionless quantity depending in general on R.

For a rough estimation one can use the spherical Bessel functions for $R_{n,l}(r)$ (further such wave functions will be called "the Bessel wave functions"), which is the case of one electron in an infinitely deep SQD. Then $\tilde{L}_{\mathbf{a},\mathbf{a}';\mathbf{b},\mathbf{b}'}$ is independent of R. Thus, it is remarkable for the Bessel wave functions that $(\overline{L}_{\mathbf{a},\mathbf{a}';\mathbf{b},\mathbf{b}'}R)$ is the constant parameter which characterizes the dynamic interaction of the electrons involved in the transitions $\mathbf{a}\rightleftarrows\mathbf{a}'$ and $\mathbf{b}\rightleftarrows\mathbf{b}'$ in *any* single SQD. (Note that $\overline{L}_{\mathbf{a},\mathbf{a}';\mathbf{b},\mathbf{b}'}R$ depends upon the dielectric constant.) This approximation also allows us to anticipate the decreasing behavior of the DE in a single SQD with growing dot radius, which is confirmed by our numerical calculations. Note that for infinitely deep SQDs with one electron the interlevel spacing behaves as R^{-2}. Then, by Eq. (15), the ratio of the absolute value of the DE shift to the interlevel gap increases with growing size of single QD.

2. A two-dimensional lattice of spherical quantum dots

Now we extend our treatment to the case of the interlevel electromagnetic response of a two-dimensional rectangular (nontunneling) lattice of spherical quantum dots (2DRLSQDs) with the translation vectors $\mathbf{d}_1$ and $\mathbf{d}_2$. The wave function describing lattice state $\overline{\mathbf{a}}$ [associated with SQD state $\mathbf{a}=(n,l,m)$] can be written in the tight-binding form

$$\Phi_{\overline{\mathbf{a}}}(\mathbf{r})=\frac{1}{N^{1/2}}\sum_{n_1,n_2}\Psi_{\mathbf{a}}(x_1-n_1d_1,x_2-n_2d_2,x_3)e^{ik_1^a n_1 d_1}e^{ik_2^a n_2 d_2}, \tag{16}$$

where $\overline{\mathbf{a}}=(\mathbf{a},\mathbf{k}_\parallel^a)$, $\mathbf{k}_\parallel^a=(k_1^a,k_2^a)$ is the wave vector of the electron at state $\overline{\mathbf{a}}$. Since we employ the periodic boundary con-

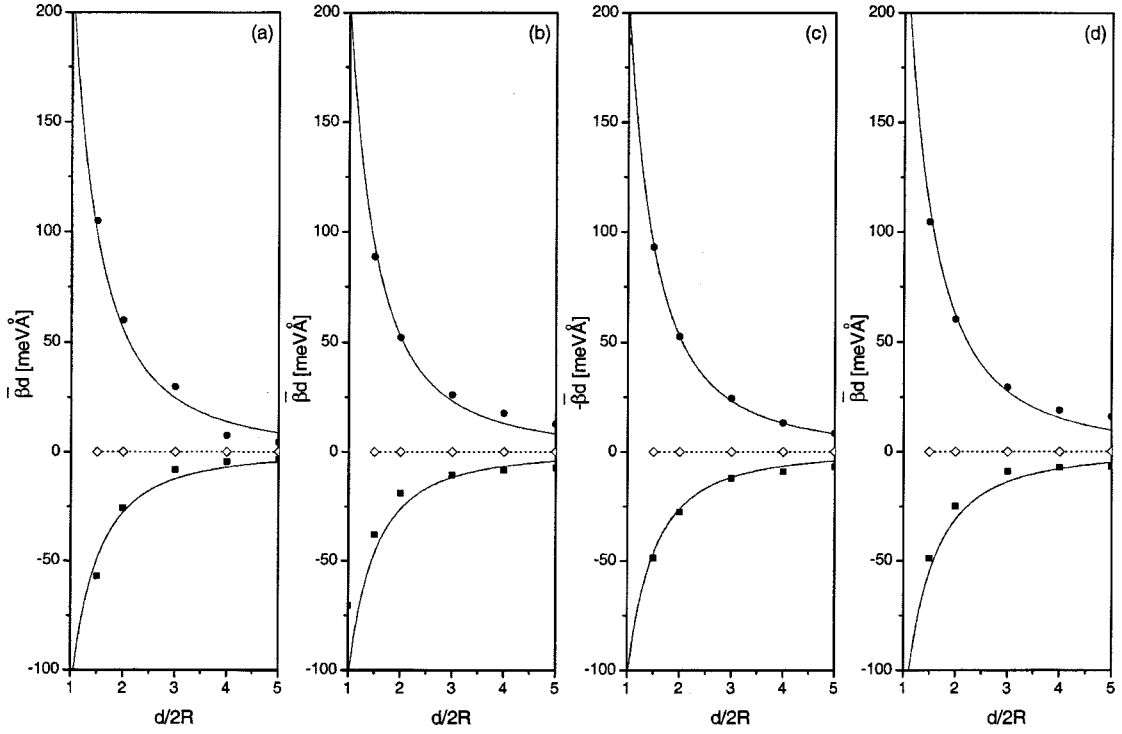

FIG. 3. Dependence of $(\overline{\beta}^{(j)}_{\mathbf{a},\mathbf{a}';\mathbf{a},\mathbf{a}'},d)$ (a), $(\overline{\beta}^{(j)}_{\mathbf{b},\mathbf{b}';\mathbf{b},\mathbf{b}'},d)$ (b), $-(\overline{\beta}^{(j)}_{\mathbf{a},\mathbf{a}';\mathbf{b},\mathbf{b}'},d)$ (c), and $(\overline{\beta}^{(j)}_{\mathbf{g},\mathbf{g}';\mathbf{g},\mathbf{g}'},d)$ (d) upon $d/2R$ for normal (circle symbols) and in-plane (square symbols) incident light polarizations for a square lattice of SQDs at $R=95$ Å with the Bessel wave functions and one electron per QD. The solid lines represent the DDA. The symbols labelling the zero level are to emphasize that the "zero" is also calculated (it is the self-interaction value).

ditions $k^a_{1(2)}=2\pi p_{1(2)}/d_{1(2)}\mathcal{N}_{1(2)}$, $\mathcal{N}_{1(2)}$ is the number of the QD rows in the $\mathbf{d}_{1(2)}$ direction and $N=\mathcal{N}_1\mathcal{N}_2$ is the number of QDs in the lattice. $n_{1(2)}$ and $p_{1(2)}$ are integers with $-\mathcal{N}_{1(2)}/2\leqslant n_{1(2)},p_{1(2)}\leqslant\mathcal{N}_{1(2)}/2$. The number N is assumed to be big enough to let any summation over the lattice sites go to infinity.

Writing Eq. (16) we have assumed that the influence of the long-range interdot static Coulomb interaction on the interlevel spacing and eigenfunctions of SQDs can be neglected as a first approximation in our approach (see Appendix A). Thus, (normalized) $\Psi_{\mathbf{a}}(\mathbf{r})$ appearing in Eq. (16) is given by Eqs. (6) and (7) derived for an isolated SQD. The normalization of the wave functions $\Phi_{\overline{\mathbf{a}}}(\mathbf{r})$ requires $\delta_{\mathbf{k}^a_\parallel-\mathbf{k}^{a'}_\parallel,\mathbf{G}_{\mathbf{m}_\parallel}}$, where $\mathbf{G}_{\mathbf{m}_\parallel}=(m_1 2\pi/d_1,m_2 2\pi/d_2)$ is the reciprocal lattice vector, $\mathbf{m}_\parallel=(m_1,m_2)$, and $m_{1(2)}$ is an integer, with $-\mathcal{N}_{1(2)}/2\leqslant m_{1(2)}\leqslant\mathcal{N}_{1(2)}/2$. The presence of $\delta_{\mathbf{k}^a_\parallel-\mathbf{k}^{a'}_\parallel,\mathbf{G}_{\mathbf{m}_\parallel}}$ means that the wave vector is conserved within the reciprocal lattice vector $\mathbf{G}_{\mathbf{m}_\parallel}$ due to periodicity of the system, and $\overline{\mathbf{a}'}=\overline{\mathbf{a}'}_{\mathbf{m}_\parallel}\equiv(\mathbf{a}',\mathbf{k}^a_\parallel+\mathbf{G}_{\mathbf{m}_\parallel})$.

Employing Eq. (16) one can check that the matrix element $(x_j)_{\overline{\mathbf{a}},\overline{\mathbf{a}'}}\equiv(\mathbf{e}_j\mathbf{r})_{\overline{\mathbf{a}},\overline{\mathbf{a}'}}$ can be written in the form

$$(x_j)_{\overline{\mathbf{a}},\overline{\mathbf{a}'}}=z_{\mathbf{a},\mathbf{a}'}\delta_{\mathbf{k}^a_\parallel-\mathbf{k}^{a'}_\parallel,\mathbf{G}_{\mathbf{m}_\parallel}}. \tag{17}$$

Inspection of the above equation shows that the dipole selection rules in the nontunneling SQD lattices are the same as in an isolated SQD given by Eq. (8).

Now the direct application of Eq. (3) let us obtain $\rho^{(1,j)}_{\overline{\mathbf{a}},\overline{\mathbf{a}'}}(\omega)$ by setting $\nu=\overline{\mathbf{a}}$ and $\nu'=\overline{\mathbf{a}'}$. Then $V^{(j)}_{\overline{\mathbf{a}},\overline{\mathbf{a}'}}(\omega)$ is the matrix element of the perturbing potential $V^{(j)}(\mathbf{r},\omega)$ and $\Gamma_{\overline{\mathbf{a}},\overline{\mathbf{a}'}}$ is the broadening parameter associated with $\overline{\mathbf{a}}\to\overline{\mathbf{a}'}$ transitions. In the further discussion, we assume for simplicity that $\Gamma_{\overline{\mathbf{a}},\overline{\mathbf{a}'}}=\Gamma_{\mathbf{a},\mathbf{a}'}$. It is important that for the lattice with a fixed number of electrons (at the states $\mathbf{a}$ and $\mathbf{a}'$) per dot we can write $\Sigma_{\mathbf{k}^{a'}_\parallel,\mathbf{k}^a_\parallel}\rho_{\overline{\mathbf{a}},\overline{\mathbf{a}'}}\delta_{\mathbf{k}^a_\parallel-\mathbf{k}^{a'}_\parallel,\mathbf{G}_{\mathbf{m}_\parallel}}=N\rho_{\mathbf{a},\mathbf{a}'}$.

To facilitate work with $\rho^{(1,j)}_{\overline{\mathbf{a}},\overline{\mathbf{a}'}}(\omega)$ we make the following reasonable assumptions. Since we neglect interdot electron tunneling in the lattice the energy of state $\overline{\mathbf{a}}$ does not depend on $\mathbf{k}^a_\parallel$, i.e., $E_{\overline{\mathbf{a}}}=E_{\mathbf{a}}\equiv E_{n,l}$ and, thus, $E_{\overline{\mathbf{a}},\overline{\mathbf{a}'}}=E_{\mathbf{a},\mathbf{a}'}$. As the following calculations show $V^{(j)}_{\overline{\mathbf{a}},\overline{\mathbf{a}'}}(\omega)$ is also independent of $\mathbf{k}^a_\parallel$ and $\mathbf{G}_{\mathbf{m}_\parallel}$, and $V^{(j)}_{\overline{\mathbf{a}},\overline{\mathbf{a}'}}(\omega)=V^{(j)}_{\mathbf{a},\mathbf{a}'}(\omega)$ [see Eq. (25)].

Taking into account the above assumptions and employing Eq. (1) we find that (effective) polarizability of the QD located in the lattice (containing N interacting QDs) $\alpha_{jj}(\omega)=\overline{\alpha}_{jj}(\omega)/N$ can be rewritten in the form

$$\alpha_{jj}(\omega)=\frac{-e}{\widetilde{E}_j(\omega)}\sum_{\mathbf{a},\mathbf{a}'}\tilde{\rho}^{(1,j)}_{\mathbf{a}',\mathbf{a}}(\omega)z_{\mathbf{a},\mathbf{a}'}, \tag{18}$$

with

$$\tilde{\rho}^{(1,j)}_{\mathbf{a},\mathbf{a}'}(\omega)\equiv\frac{1}{N}\sum_{\mathbf{k}^a_\parallel,\mathbf{k}^{a'}_\parallel}\delta_{\mathbf{k}^a_\parallel-\mathbf{k}^{a'}_\parallel,\mathbf{G}_{\mathbf{m}_\parallel}}\rho^{(1,j)}_{\overline{\mathbf{a}},\overline{\mathbf{a}'}}(\omega)=\frac{V^{(j)}_{\mathbf{a},\mathbf{a}'}(\omega)n_{\mathbf{a},\mathbf{a}'}}{E_{\mathbf{a},\mathbf{a}'}-\hbar\omega-i\Gamma_{\mathbf{a},\mathbf{a}'}}. \tag{19}$$

The perturbing potential (inside a particular QD) is the sum of the external perturbing potential and the potential induced due to the intradot and interdot dynamic *e-e* interaction [see Eq. (4)]. To properly take into account the interdot *e-e* interaction it is convenient to have each lattice site labeled by (l,k), where l and k are the integers. The site (0,0) contains the origin of the coordinate system. The radius-vector to the volume associated with the (l,k)th SQD is denoted by $\tilde{\mathbf{r}}'_{lk}$. Then

$$V^{(j)\mathrm{ind}}(\mathbf{r},\omega)=\frac{e^2}{4\pi\epsilon\epsilon_0}\sum_{l,k=-\infty}^{\infty}\int d\tilde{\mathbf{r}}'_{lk}\frac{1}{|\mathbf{r}-\tilde{\mathbf{r}}'_{lk}|}\sum_{\overline{\mathbf{b}},\overline{\mathbf{b}'}}\rho^{(1,j)}_{\overline{\mathbf{b}},\overline{\mathbf{b}'}}(\omega)\times\Phi^{*}_{\overline{\mathbf{b}'}}(\tilde{\mathbf{r}}'_{lk})\Phi_{\overline{\mathbf{b}}}(\tilde{\mathbf{r}}'_{lk}). \tag{20}$$

Note that the summation includes the term with $l=0$ and $k=0$ which represents the intradot *e-e* interaction. Consequently, the problem of the self-interaction of one electron in a QD with itself appears. It is important to note that Eq. (20) represents the *existing* potential; the self-interaction does not matter yet. The self-interaction problem arises when we calculate the matrix elements of $V^{(j)}(\mathbf{r},\omega)$ for the potential *experienced* by an electron (see Sec. II A 1). So this self-interaction problem will be addressed further.

Now, by using the vector $\mathbf{R}_{lk}=(ld_1,kd_2,0)$, we introduce the radius vector $\mathbf{r}'=\tilde{\mathbf{r}}'_{lk}-\mathbf{R}_{lk}$ which is originated in the center of the (l,k)th SQD. Employing the 2D Fourier transform in the x_1-x_2 plane of the periodic lattice

$$\frac{1}{|\mathbf{r}-\tilde{\mathbf{r}}'_{lk}|}=\frac{1}{|\mathbf{r}-(\mathbf{r}'+\mathbf{R}_{lk})|}=\frac{2\pi}{S}\sum_{\mathbf{q}_\parallel}e^{i\mathbf{q}_\parallel\mathbf{d}_{lk}}\frac{1}{q_\parallel}e^{-q_\parallel|x_3-x'_3|}e^{-i\mathbf{q}_\parallel(\mathbf{r}_\parallel-\mathbf{r}'_\parallel)}, \tag{21}$$

we can rewrite Eq. (20) in the following form:

$$V^{(j)\mathrm{ind}}(\mathbf{r},\omega)=\frac{e^2}{2\epsilon\epsilon_0 S}\sum_{\mathbf{q}_\parallel}\sum_{l,k=-\infty}^{\infty}e^{i\mathbf{q}_\parallel\mathbf{d}_{lk}}\frac{1}{q_\parallel}e^{-i\mathbf{q}_\parallel\mathbf{r}_\parallel}\times\int dx'_3e^{-q_\parallel|x_3-x'_3|}\sum_{\overline{\mathbf{b}},\overline{\mathbf{b}'}}F^{(j)+}_{\overline{\mathbf{b}'},\overline{\mathbf{b}}}(\mathbf{q}_\parallel,x'_3)\rho^{(1,j)}_{\overline{\mathbf{b}},\overline{\mathbf{b}'}}(\omega), \tag{22}$$

where $\mathbf{d}_{lk}=(ld_1,kd_2)$. The vector $\mathbf{q}_\parallel=(q_1,q_2)$, having dimension of reciprocal length, can be considered as the wave vector of the collective excitation associated with interlevel transitions.

The form factor $F^{(j)+}_{\overline{\mathbf{b}'},\overline{\mathbf{b}}}(\mathbf{q}_\parallel,x_3)$ is defined by

$$F^{(j)+}_{\overline{\mathbf{b}'},\overline{\mathbf{b}}}(\mathbf{q}_\parallel,x_3)=\int d\mathbf{r}_\parallel\Phi^{*}_{\overline{\mathbf{b}'}}(\mathbf{r})\Phi_{\overline{\mathbf{b}}}(\mathbf{r})e^{i\mathbf{q}_\parallel\mathbf{r}_\parallel}. \tag{23}$$

In Eq. (22) we take the advantage of the summation over (l,k) as $\Sigma^{\infty}_{l,k=-\infty}e^{i\mathbf{q}_\parallel\mathbf{d}_{lk}}=N\delta_{\mathbf{q}_\parallel\mathbf{d}_{lk},0}$ which imposes the periodic boundary conditions on $\mathbf{q}_\parallel$, so that, in effect, $\mathbf{q}_\parallel=\mathbf{G}_{\mathbf{m}_\parallel}$. Thus, we conclude that in the approximation used here, i.e., when $\mathbf{E}^{\mathrm{ext}}(\mathbf{r},t)=\mathbf{e}_j\tilde{E}_j(\omega)e^{-i\omega t}$, only the collective excitations with $\mathbf{q}_\parallel=\mathbf{G}_{\mathbf{m}_\parallel}$ can be excited by the external radiation.

For the form factor we find that $F^{(j)\pm}_{\overline{\mathbf{b}'},\overline{\mathbf{b}}}(\mathbf{G}_{\mathbf{m}_\parallel},x_3)=\delta_{\mathbf{k}^{b'}_\parallel-\mathbf{k}^{b}_\parallel,\pm\mathbf{G}_{\mathbf{m}_\parallel}}F^{(j)\pm}_{\mathbf{b}',\mathbf{b}}(\mathbf{G}_{\mathbf{m}_\parallel},x_3)$, with

$$F^{(j)\pm}_{\mathbf{b}',\mathbf{b}}(\mathbf{G}_{\mathbf{m}_\parallel},x_3)=\int d\mathbf{r}_\parallel\Psi^{*}_{\mathbf{b}'}(\mathbf{r}_\parallel,x_3)e^{\pm i\mathbf{G}_{\mathbf{m}_\parallel}\mathbf{r}_\parallel}\Psi_{\mathbf{b}}(\mathbf{r}_\parallel,x_3). \tag{24}$$

In Eq. (24) the integration is carried out over one SQD which is possible due to the periodicity of the wave function according to Eq. (16).

Then, taking the matrix element of $V^{(j)\mathrm{ind}}(\mathbf{r},\omega)$ between states $\overline{\mathbf{a}}$ and $\overline{\mathbf{a}'}=\overline{\mathbf{a}'_{\mathbf{m}_\parallel}}$ we get

$$V^{(j)\mathrm{ind}}_{\overline{\mathbf{a}},\overline{\mathbf{a}'}}(\omega)\equiv V^{(j)\mathrm{ind}}_{\mathbf{a},\mathbf{a}'}(\omega)=\sum_{\mathbf{b},\mathbf{b}'}\beta^{(j)}(\mathbf{a},\mathbf{a}';\mathbf{b},\mathbf{b}')\tilde{\rho}^{(1,j)}_{\mathbf{b},\mathbf{b}'}(\omega), \tag{25}$$

where

$$\beta^{(j)}(\mathbf{a},\mathbf{a}';\mathbf{b},\mathbf{b}')=\frac{e^2}{2\epsilon\epsilon_0 d_1d_2}\sum_{\mathbf{G}_{\mathbf{m}_\parallel}}\frac{1}{G_{\mathbf{m}_\parallel}}\int dx_3dx'_3e^{-G_{\mathbf{m}_\parallel}|x_3-x'_3|}\times F^{(j)-}_{\mathbf{a},\mathbf{a}'}(\mathbf{G}_{\mathbf{m}_\parallel},x_3)F^{(j)+}_{\mathbf{b}',\mathbf{b}}(\mathbf{G}_{\mathbf{m}_\parallel},x'_3), \tag{26}$$

and $G_{\mathbf{m}_\parallel}=|\mathbf{G}_{\mathbf{m}_\parallel}|$. Here the relation $N/S=d_1d_2$ is used. One can check that $\beta^{(j)}(\mathbf{c},\mathbf{c}';\mathbf{c},\mathbf{c}')>0$ and $\beta^{(j)}(\mathbf{a},\mathbf{a}';\mathbf{b},\mathbf{b}')<0$ if $\mathbf{a}\neq\mathbf{b}$ and/or $\mathbf{a}'\neq\mathbf{b}'$ for the lattice of spherical QDs.

It should also be noted that the exponential factor $e^{-G_{\mathbf{m}_\parallel}|x_3-x'_3|}$ in Eq. (26) appears because the two-dimensional lattice is built by the three-dimensional quantum dots; more precisely, the QDs have nonzero size in the direction $\mathbf{e}_3$ normal to the plane of the lattice. One can suggest that when this size of the dot becomes comparable with d_1 and/or d_2, the presence of the exponential factor in some situations could impact the strength of the dynamic long-range Coulomb interaction in the lattice.

We find from Eqs. (19), (25), and (26) that $\tilde{\rho}^{(1,j)}_{\mathbf{a},\mathbf{a}'}(\omega)$ is defined by Eq. (5) if $\nu=\mathbf{a}$, $\nu'=\mathbf{a}'$ $\sigma=\mathbf{b}$, $\sigma'=\mathbf{b}'$, $\varrho^{(1,j)}_{\nu\nu'}(\omega)=\tilde{\rho}^{(1,j)}_{\mathbf{a},\mathbf{a}'}(\omega)$, $\mathcal{L}^{(j)}(\nu,\nu';\sigma,\sigma')=\beta^{(j)}(\mathbf{a},\mathbf{a}';\mathbf{b},\mathbf{b}')$, and $\mathcal{N}_{\nu\nu'}=n_{\mathbf{a},\mathbf{a}'}$.

Now the problem of the self-interaction should be figured out. Equations (25) and (26) represent the potential experienced by a certain electron in a certain QD of the lattice due to interaction of that electron with all the electrons in the lattice. Thus, this potential includes the interdot *e-e* interaction as well as the intradot *e-e* interaction. It is important to note that these two contributions cannot be separated in Eqs. (25) and (26). The interdot interaction is described correctly by these equations for any number of electrons per dot. However, Eqs. (25) and (26) do include the self-interaction of an electron through the intradot *e-e* interaction as is described in Sec. II A 1 for a single SQD. Thus, this self-interaction contribution to the DE shift is calculated separately by Eq. (13) and then subtracted from the value of the DE shift given by Eq. (26). Note that this way of solution of the self-interaction problem is justified within our approximation when the electron eigenstates in the QDs are assumed to be untouched by the static interdot *e-e* interaction.

An analysis of the obtained relationships reveals very important general features of the depolarization effect in systems of quantum dots which allows us to solve the problem of the electron self-interaction. First of all, comparing the relationships for the case of a single SQD in Sec. II A 1 and the above relationships for the lattice one can see that they are strongly related. In fact, the relationships for the lattice are transformed into the corresponding relationships for single dot, in part Eq. (26) is rendered into Eq. (11), when the step of the summation over $\mathbf{G}_{\mathbf{m}_\parallel}$ is sufficiently small so that the summation limits the integration. Since this limit is realized when $d_l \to \infty$, it means that the DE in the lattice with a sufficiently large d_l comes close to the DE in a single SQD. Our numerical calculations confirm that for any direction $\mathbf{e}_j$ of the radiation polarization

$$\lim_{d/2R\to\infty} \beta^{(j)}(\mathbf{a},\mathbf{a}';\mathbf{b},\mathbf{b}') = L(\mathbf{a},\mathbf{a}';\mathbf{b},\mathbf{b}'). \tag{27}$$

For simplicity we consider a square lattice with $d=d_1=d_2$ in the further analysis. Inspection of the obtained results (see also Sec. II B) indicates that strength of the DE shift is controlled not only by the factors $\beta^{(j)}(\mathbf{a},\mathbf{a}';\mathbf{b},\mathbf{b}')$ themselves but rather by products $\beta^{(j)}_{\mathbf{a},\mathbf{a}';\mathbf{b},\mathbf{b}'}=\beta^{(j)}(\mathbf{a},\mathbf{a}';\mathbf{b},\mathbf{b}')\sqrt{n_{\mathbf{a},\mathbf{a}'}n_{\mathbf{b},\mathbf{b}'}}$. When $\mathbf{a}=\mathbf{b}$ and $\mathbf{a}'=\mathbf{b}'$ (and $n_{\mathbf{a},\mathbf{a}'}\geqslant 1$) this is the case of the self-interaction and, consequently, $\beta^{(j)}_{\mathbf{a},\mathbf{a}';\mathbf{a},\mathbf{a}'}$ contains the self-interaction contribution. However, when we consider only the coupling between different transitions, i.e., when $\mathbf{a}\neq\mathbf{b}$ and/or $\mathbf{a}'\neq\mathbf{b}'$ (and $n_{\mathbf{a},\mathbf{a}'}, n_{\mathbf{b},\mathbf{b}'}\geqslant 1$) this is *not* the case of the self-interaction.

It is important to mention the case of only a single electron per QD which occupies a degenerated level [such as $(1,1,m)$ in SQD] so that this one electron can be at state $\mathbf{a}$ or $\mathbf{b}$ [(1, 1, 0) or $(1,1,\pm 1)$ in SQD] with different probabilities. Consequently, the one electron can participate in transitions of *different* types, $\mathbf{a}\rightleftarrows\mathbf{a}'$ and $\mathbf{b}\rightleftarrows\mathbf{b}'$, with different probabilities. Then we can calculate $\beta^{(j)}_{\mathbf{a},\mathbf{a}';\mathbf{b},\mathbf{b}'}$ which includes *no* self-interaction contribution.

The above discussion suggests that the effects associated with self-interaction can be excluded replacing $\beta^{(j)}_{\mathbf{a},\mathbf{a}';\mathbf{b},\mathbf{b}'}$ by

$$\overline{\beta}^{(j)}_{\mathbf{a},\mathbf{a}';\mathbf{b},\mathbf{b}'} = [\beta^{(j)}(\mathbf{a},\mathbf{a}';\mathbf{b},\mathbf{b}') - L(\mathbf{a},\mathbf{a}';\mathbf{a},\mathbf{a}')\delta_{\mathbf{a},\mathbf{b}}\delta_{\mathbf{a}',\mathbf{b}'}]\sqrt{n_{\mathbf{a},\mathbf{a}'}n_{\mathbf{b},\mathbf{b}'}}. \tag{28}$$

Note that expression for $\overline{\beta}^{(j)}_{\mathbf{a},\mathbf{a}';\mathbf{b},\mathbf{b}'}$ can be rewritten in a form analogous to Eq. (15) as

$$\overline{\beta}^{(j)}_{\mathbf{a},\mathbf{a}';\mathbf{b},\mathbf{b}'} = \frac{e^2}{\epsilon\epsilon_0 d}\tilde{\beta}^{(j)}_{\mathbf{a},\mathbf{a}';\mathbf{b},\mathbf{b}'}, \tag{29}$$

where $\tilde{\beta}^{(j)}_{\mathbf{a},\mathbf{a}';\mathbf{b},\mathbf{b}'}$ is a dimensionless function of d and R. In the case of the infinite barrier (the Bessel wave functions) $\tilde{\beta}^{(j)}_{\mathbf{a},\mathbf{a}';\mathbf{b},\mathbf{b}'}$ depends only on the ratio $d/2R$.

It is very important to note that the term with $\mathbf{G}_{\mathbf{m}_\parallel}=0$ in Eq. (26) is determining the radical difference between the DE shift for the normal and in-plane light polarization: the contribution of the interdot *e-e* interaction into the DE shift is positive for the normal light polarization and negative for the in-plane light polarization. (We assume that the self-interaction is excluded.)

At this point we would like to emphasize that the relationships obtained in this subsection are general and can be applied to the 2D rectangular nontunneling lattice of identical quantum dots of other shape and size. The shape of the dots is taken into account by Eq. (24).

B. Interlevel optical response of quantum dot systems

Now we are able to find out explicit expressions for $\boldsymbol{\alpha}$, which describes the effective polarizability of a QD in the lattice as well as the polarizability of single QD, by applying Eqs. (1) and (5). In the following the diagonal components of $\boldsymbol{\alpha}$ are obtained for two-state and four-state electron systems which can be realized depending upon the number of electrons per dot. The course of the development is identical for the single QD and for the lattice. As has been mentioned in the former case the polarizability tensor reduces to scalar $\alpha_{jj}=\alpha$, i.e., it is independent on the light polarization. To unify the final relationships we introduce the quantity $\mathcal{B}^{(j)}(\mathbf{a},\mathbf{a}';\mathbf{b},\mathbf{b}')$ which takes the value of $L(\mathbf{a},\mathbf{a}';\mathbf{b},\mathbf{b}')$ or $\beta^{(j)}(\mathbf{a},\mathbf{a}';\mathbf{b},\mathbf{b}')$ for the single QD or the lattice, respectively. Moreover, we also define $\overline{\mathcal{B}}^{(j)}_{\mathbf{a},\mathbf{a}';\mathbf{b},\mathbf{b}'}$ to be $\overline{L}_{\mathbf{a},\mathbf{a}';\mathbf{b},\mathbf{b}'}$ or $\overline{\beta}^{(j)}_{\mathbf{a},\mathbf{a}';\mathbf{b},\mathbf{b}'}$, correspondingly.

For further analysis the following symmetry relations for the spherical QDs are important: $\mathcal{B}^{(j)}(\mathbf{a},\mathbf{a}';\mathbf{b},\mathbf{b}')=\mathcal{B}^{(j)}(\mathbf{b},\mathbf{b}';\mathbf{a},\mathbf{a}')$, $\mathcal{B}^{(j)}(\mathbf{a},\mathbf{a}';\mathbf{b},\mathbf{b}')=\mathcal{B}^{(j)}(\mathbf{a}',\mathbf{a};\mathbf{b}',\mathbf{b})$, and $\mathcal{B}^{(j)}(\mathbf{a},\mathbf{a}';\mathbf{b},\mathbf{b}')=-\mathcal{B}^{(j)}(\mathbf{a},\mathbf{a}';\mathbf{b}',\mathbf{b})$, $\mathcal{B}^{(j)}(\mathbf{a},\mathbf{a}';\mathbf{b},\mathbf{b}')=-\mathcal{B}^{(j)}(\mathbf{a}',\mathbf{a};\mathbf{b},\mathbf{b}')$. Note also that $\mathcal{B}^{(j)}(\mathbf{c},\mathbf{c}';\mathbf{c},\mathbf{c}')>0$ and $\mathcal{B}^{(j)}(\mathbf{a},\mathbf{a}';\mathbf{b},\mathbf{b}')<0$ if $\mathbf{a}\neq\mathbf{b}$ and/or $\mathbf{a}'\neq\mathbf{b}'$.

We would like to stress that to simplify the further consideration we assume that the broadening parameter is independent of the level index, i.e., $\Gamma_{\nu'\nu}\equiv\Gamma$, with Γ taken as a phenomenological parameter. Discussion of other situations when the level index is important for the broadening parameter is beyond the scope of this paper.

1. Two-state electron system

Let us consider a pair of levels $\mathbf{a}$ and $\mathbf{a}'$ ($E_{\mathbf{a}'}>E_{\mathbf{a}}$ and $n_{\mathbf{a},\mathbf{a}'}>0$) between which dipole transitions are allowed. Note, that the $\mathbf{a}'\to\mathbf{a}$ transition can be resonant (if $\hbar\omega\approx E_{\mathbf{a}',\mathbf{a}}$) while the $\mathbf{a}\to\mathbf{a}'$ transition is always nonresonant. We call the collective mode associated with the $\mathbf{a}\rightleftarrows\mathbf{a}'$ transitions as the *a* mode. If we neglect another transition (the diagonal approximation) then the direct calculations show that the polarizability can be written in the following form:

$$\alpha_{jj}(\omega) = \frac{2|\mu_{\mathbf{a}',\mathbf{a}}|^2 n_{\mathbf{a},\mathbf{a}'}E_{\mathbf{a}',\mathbf{a}}}{(\tilde{E}^{(j)}_{\mathbf{a}',\mathbf{a}})^2 - (\hbar\omega)^2 - i2\hbar\omega\Gamma}, \tag{30}$$

where $\mu_{\mathbf{a}',\mathbf{a}}=-ez_{\mathbf{a}',\mathbf{a}}$ is matrix element of the electron dipole moment and

$$(\tilde{E}^{(j)}_{\mathbf{a}',\mathbf{a}})^2 = E^2_{\mathbf{a}',\mathbf{a}} + 2E_{\mathbf{a}',\mathbf{a}}\overline{\mathcal{B}}^{(j)}_{\mathbf{a},\mathbf{a}',\mathbf{a},\mathbf{a}'}. \tag{31}$$

In Eq. (30) Γ^2 is omitted in the denominator since $\Gamma^2 \ll (\tilde{E}^{(j)}_{\mathbf{a}',\mathbf{a}})^2$.

Thus, we see that in the diagonal limit the dynamic *e-e* interaction affects only the resonant energy. If we neglect this interaction then $\tilde{E}^{(j)}_{\mathbf{a}',\mathbf{a}}=E_{\mathbf{a}',\mathbf{a}}$ and the above expression reduces to the well known one-electron expression (see, e.g., Ref. 21).

The imaginary part of $\alpha_{jj}(\omega)$ can be written in the form

$$\alpha''_{jj}(\omega)=\frac{4|\mu_{\mathbf{a}',\mathbf{a}}|^2 n_{\mathbf{a},\mathbf{a}'}E_{\mathbf{a}',\mathbf{a}}\hbar\omega\Gamma}{[(\tilde{E}^{(j)}_{\mathbf{a}',\mathbf{a}})^2-(\hbar\omega)^2]^2+(2\hbar\omega\Gamma)^2}. \tag{32}$$

When only the resonant transitions are taken into account (the resonant approximation) and $|\bar{\mathcal{B}}^{(j)}_{\mathbf{a},\mathbf{a}',\mathbf{a},\mathbf{a}'}|\ll E_{\mathbf{a}',\mathbf{a}}$ the above equation simplifies to the form

$$\alpha''_{jj}(\omega)=\frac{|\mu_{\mathbf{a}',\mathbf{a}}|^2 n_{\mathbf{a},\mathbf{a}'}\Gamma}{(\bar{E}^{(j)}_{\mathbf{a}',\mathbf{a}}-\hbar\omega)^2+\Gamma^2}, \tag{33}$$

where $\bar{E}^{(j)}_{\mathbf{a}',\mathbf{a}}=E_{\mathbf{a}',\mathbf{a}}+\bar{\mathcal{B}}^{(j)}_{\mathbf{a},\mathbf{a}',\mathbf{a},\mathbf{a}'}$.

It should be noted that $\tilde{E}^{(j)}_{\mathbf{a}',\mathbf{a}}>E_{\mathbf{a}',\mathbf{a}}$ and $\bar{E}^{(j)}_{\mathbf{a}',\mathbf{a}}>E_{\mathbf{a}',\mathbf{a}}$ in case of normal occupation of the levels ($n_{\mathbf{a},\mathbf{a}'}>0$), except $\tilde{E}^{(j)}_{\mathbf{a}'\mathbf{a}}<E_{\mathbf{a}'\mathbf{a}}$ and $\bar{E}^{(j)}_{\mathbf{a}'\mathbf{a}}<E_{\mathbf{a}'\mathbf{a}}$ for the lattice, in-plane light polarization (i.e., $j=1,2$), and $n_{\mathbf{aa}'}=1$ (see Fig. 1).

The considered above two-state approximation is valid only when electron transitions between two bound states play dominant role for a given photon energy. For example, such a situation takes place when electrons are excited from the occupied lowest state of SQD, $\mathbf{a}=(1,0,0)$, to the first (empty) excited state $\mathbf{a}'=(1,1,0)$ and simultaneously $\hbar\omega\approx E_{1,1}-E_{1,0}$. It is important to note that in a single QD the lowest state (1,0,0) must be occupied by two electrons whose transitions form the collective excitation (the *a* mode) due to the intradot *e-e* interaction. On the other hand, at least one electron per dot is required for the lattice where the *a* mode of the collective lattice excitation is formed due to the interdot *e-e* interaction.

2. Four-state electron system

Now we consider a system of four states, namely, **a** and $\mathbf{a}'$ ($E_{\mathbf{a}'}>E_{\mathbf{a}}$ and $n_{\mathbf{a},\mathbf{a}'}>0$), and **b** and $\mathbf{b}'$ ($E_{\mathbf{b}'}>E_{\mathbf{b}}$ and $n_{\mathbf{b},\mathbf{b}'}>0$), with the allowed dipole transitions are $\mathbf{a}\rightleftarrows\mathbf{a}'$ (the *a* mode) and $\mathbf{b}\rightleftarrows\mathbf{b}'$ (the *b* mode) only. In the diagonal limit the four-state system reduces to two noninteracting two-state systems describing the *a* and *b* modes separately. When coupling between the above modes is taken into account the polarizability can be written as

$$\alpha_{jj}(\omega)=\frac{-e}{\tilde{E}_j(\omega)}[\bar{\rho}^{(1,j)}_{\mathbf{a}',\mathbf{a}}(\omega)(x_j)_{\mathbf{a},\mathbf{a}'}+\bar{\rho}^{(1,j)}_{\mathbf{b}',\mathbf{b}}(\omega)(x_j)_{\mathbf{b},\mathbf{b}'}], \tag{34}$$

where $\bar{\rho}^{(1,j)}_{\mathbf{c}',\mathbf{c}}(\omega)=\tilde{\rho}^{(1,j)}_{\mathbf{c}',\mathbf{c}}(\omega)-\tilde{\rho}^{(1,j)}_{\mathbf{c},\mathbf{c}'}(\omega)$.

Application of Eq. (5) to the four-level model gives sets of two equations for $\bar{\rho}^{(1,j)}_{\mathbf{a}',\mathbf{a}}(\omega)$ and $\bar{\rho}^{(1,j)}_{\mathbf{b}',\mathbf{b}}(\omega)$. Substituting the solutions of these equations into Eq. (34) we get

$$\alpha_{jj}(\omega)=e^2\frac{-[A_j(\omega)+iB_j(\omega)]}{[(\hbar\omega^{(j)}_{-})^2+\Gamma^2-(\hbar\omega)^2-i2\hbar\omega\Gamma][(\hbar\omega^{(j)}_{+})^2+\Gamma^2-(\hbar\omega)^2-i2\hbar\omega\Gamma]}, \tag{35}$$

where

$$\begin{aligned}A_j(\omega)=&\,2E_{\mathbf{a}',\mathbf{a}}|(x_j)_{\mathbf{a}',\mathbf{a}}|^2 n_{\mathbf{a},\mathbf{a}'}\{[(\tilde{E}^{(j)}_{\mathbf{b}',\mathbf{b}})^2+\Gamma^2]-(\hbar\omega)^2\}\\&+2E_{\mathbf{b}',\mathbf{b}}|(x_j)_{\mathbf{b}',\mathbf{b}}|^2 n_{\mathbf{b},\mathbf{b}'}\{[(\tilde{E}^{(j)}_{\mathbf{a}',\mathbf{a}})^2+\Gamma^2]-(\hbar\omega)^2\}\\&-8E_{\mathbf{a}',\mathbf{a}}E_{\mathbf{b}',\mathbf{b}}|(x_j)_{\mathbf{a}',\mathbf{a}}(x_j)_{\mathbf{b}',\mathbf{b}}\bar{\mathcal{B}}^{(j)}_{\mathbf{a},\mathbf{a}',\mathbf{b},\mathbf{b}'}|\sqrt{n_{\mathbf{a},\mathbf{a}'}n_{\mathbf{b},\mathbf{b}'}},\end{aligned} \tag{36}$$

$$B_j(\omega)=-4\hbar\omega\Gamma[E_{\mathbf{a}',\mathbf{a}}|(x_j)_{\mathbf{a}',\mathbf{a}}|^2 n_{\mathbf{a},\mathbf{a}'}+E_{\mathbf{b}',\mathbf{b}}|(x_j)_{\mathbf{b}',\mathbf{b}}|^2 n_{\mathbf{b},\mathbf{b}'}], \tag{37}$$

and

$$\begin{aligned}(\hbar\omega^{(j)}_{\pm})^2=&\,\frac{1}{2}[(\tilde{E}^{(j)}_{\mathbf{a}',\mathbf{a}})^2+(\tilde{E}^{(j)}_{\mathbf{b}',\mathbf{b}})^2]\\&\pm\frac{1}{2}\sqrt{[(\tilde{E}^{(j)}_{\mathbf{a}',\mathbf{a}})^2-(\tilde{E}^{(j)}_{\mathbf{b}',\mathbf{b}})^2]^2+16E_{\mathbf{a}',\mathbf{a}}E_{\mathbf{b}',\mathbf{b}}(\bar{\mathcal{B}}^{(j)}_{\mathbf{a},\mathbf{a}';\mathbf{b},\mathbf{b}'})^2}.\end{aligned} \tag{38}$$

The above equations clearly show that in the four level systems the intermode coupling (controlled by the parameter $\bar{\mathcal{B}}^{(j)}_{\mathbf{a},\mathbf{a}',\mathbf{b},\mathbf{b}'}$) leads to the formation of new mixed modes. In the presence of the broadening, the peak positions in the absorption spectra appear at the energies denoted by $\hbar\omega^{(j)}_{\mathrm{res}-}$ and $\hbar\omega^{(j)}_{\mathrm{res}+}$ which can be associated with the eigenenergies of the mixed modes. Our numerical simulations show that, numerical values of these energies are very close to $\hbar\omega^{(j)}_{-}$ and $\hbar\omega^{(j)}_{+}$, respectively, i.e., $\hbar\omega^{(j)}_{\mathrm{res}-}\approx\hbar\omega^{(j)}_{-}$ and $\hbar\omega^{(j)}_{\mathrm{res}+}\approx\hbar\omega^{(j)}_{+}$ (see also Fig. 7). As one can expect the above energies differ from the eigenenergies of the uncoupled modes $\tilde{E}^{(j)}_{\mathbf{a}',\mathbf{a}}$ and $\tilde{E}^{(j)}_{\mathbf{b}',\mathbf{b}}$, with

$\hbar\omega^{(j)}_{\mathrm{res}-} < \min(\tilde{E}^{(j)}_{\mathbf{a}',\mathbf{a}}, \tilde{E}^{(j)}_{\mathbf{b}',\mathbf{b}})$ and $\hbar\omega^{(j)}_{\mathrm{res}+} > \max(\tilde{E}^{(j)}_{\mathbf{a}',\mathbf{a}}, \tilde{E}^{(j)}_{\mathbf{b}',\mathbf{b}})$. Corrections induced by the mode coupling are largest when the difference between $\tilde{E}^{(j)}_{\mathbf{a}',\mathbf{a}}$ and $\tilde{E}^{(j)}_{\mathbf{b}',\mathbf{b}}$ vanishes. In this regime the separation between the low-energy peak (at $\hbar\omega^{(j)}_{\mathrm{res}-}$) and the high-energy peak (at $\hbar\omega^{(j)}_{\mathrm{res}+}$) in the spectrum of $\mathcal{P}^{(j)}$ can be approximated by

$$\Delta E^{(j)} \equiv \hbar\omega^{(j)}_{\mathrm{res}+} - \hbar\omega^{(j)}_{\mathrm{res}-} \approx \hbar\omega^{(j)}_{+} - \hbar\omega^{(j)}_{-} = 2|\overline{\mathcal{B}}^{(j)}_{\mathbf{a},\mathbf{a}',\mathbf{b},\mathbf{b}'}|. \tag{39}$$

The considered above four-state system can be used for modelling optical properties of the SQD when the two lowest energy levels [states (1, 0, 0) and $(1,1,m)$ with $m=0,-1,1$] are occupied, and the following electron transitions from states $(1,1,m)$ to vacant corresponding states $(1,2,m)$ play a dominant role: $(1,1,0)\leftrightarrows(1,2,0)$, $(1,1,1)\leftrightarrows(1,2,1)$, and $(1,1,-1)\leftrightarrows(1,2,-1)$.

One can check, employing the diagonal approximation, that the transitions $(1,1,1)\leftrightarrows(1,2,1)$ and $(1,1,-1)\leftrightarrows(1,2,-1)$ have the same matrix elements of the perturbing potential. Thus, only two kinds of the optically active transitions are distinguished: $(1,1,0)\leftrightarrows(1,2,0)$ and $(1,1,\pm1)\leftrightarrows(1,2,\pm1)$. Then it is convenient to introduce the following notation: $\mathbf{a}=(1,1,0)$, $\mathbf{a}'=(1,2,0)$, $\mathbf{b}=(1,1,\pm1)$, and $\mathbf{b}'=(1,2,\pm1)$. It should be especially emphasized that it is the high symmetry of the SQD that allows the degeneration of the energy levels, i.e., $E_{\mathbf{a}}=E_{\mathbf{b}}=E_{1,1}$, $E_{\mathbf{a}'}=E_{\mathbf{b}'}=E_{1,2}$, and consequently $E_{\mathbf{a}',\mathbf{a}}=E_{\mathbf{b}',\mathbf{b}}=E_{(1,2)(1,1)}$. Thus, the intermode coupling in such a SQD has resonant character so that we can expect a strong influence of the *e-e* coupling on the interlevel absorption spectra of the SQD. Note that in the dipole approximation no transitions from the lowest level (1,0,0) are possible: to the second level due to the Pauli principle and to the third level due to the selection rule $\Delta l=1$.

It is also important to stress that the coupling (due to V^{ind}) between the considered above dipole active modes and optically inactive modes (associated with $\mathbf{a}\leftrightarrows\mathbf{b}'$ and $\mathbf{b}\leftrightarrows\mathbf{a}'$ transitions) does not play any role since $\mathcal{B}^{(j)}_{\mathbf{a},\mathbf{a}';\mathbf{a}',\mathbf{b}} = \mathcal{B}^{(j)}_{\mathbf{b},\mathbf{b}';\mathbf{b}',\mathbf{a}} \equiv 0$. Working in the four level model we neglect the coupling between the dipole transitions ($\Delta l=1$) and multipole excitations ($\Delta l \geqslant 2$). It has a good justification because in the structures considered here the (single electron) resonant energies corresponding to the dipole transitions ($E_{\mathbf{a}',\mathbf{a}}=E_{\mathbf{b}',\mathbf{b}}$) and multipole transitions ($E_{1,\Delta l}-E_{1,0}$) differ strongly.

3. Modified oscillator strength approach

Inspection of Eq. (35) shows that it is very complicated for analysis and allows us to get information about the influence of the intermode coupling on the height of the absorption peaks only by means of the numerical calculations. This complexity is mainly caused by rigorous treatment of the broadening even if the dependence of $\Gamma_{\mathbf{a},\mathbf{a}'}$ on the level index is neglected for simplicity (i.e., $\Gamma_{\mathbf{a},\mathbf{a}'}=\Gamma$). Fortunately, it is the concept of the modified oscillator strength (MOS) that let us drastically simplify and enhance the analysis (see, e.g., Ref. 28).

In this section we are going to exploit the concept of the MOS. Comparison of the exact relationship for the polarizability and that obtained in the MOS approach [namely, Eqs. (35) and (46)] enables us to estimate the applicability of the MOS approach. To the best of our knowledge such a comparison and application of the concept of the MOS to QD systems have not been discussed in the literature.

The MOS concept is based on the assumption that broadening parameter Γ is much smaller than the uncoupled mode energy. Modeling each peak on the spectra by the δ functions, i.e., when $\Gamma=0$, the polarizability of the multimode system is presented by a very compact general expression

$$\alpha_{jj}(\omega) = \frac{e^2\hbar^2}{m_0}\sum_{\eta}\frac{\tilde{f}^{(j)}_{\eta}}{(\hbar\omega^{(j)}_{\eta})^2 - (\hbar\omega)^2}, \tag{40}$$

where $\tilde{f}^{(j)}_{\eta}$ is the modified oscillator strength corresponding to the ηth eigenenergy.

Applying the MOS concept to the case of the four-state system considered here the relationships for the modified oscillator strength $\tilde{f}^{(j)}_{-}$ and $\tilde{f}^{(j)}_{+}$ associated with the eigenenergies $\hbar\omega^{(j)}_{-}$ and $\hbar\omega^{(j)}_{+}$, respectively, are obtained with the help of Eq. (35) in a very simple form

$$\tilde{f}^{(j)}_{-} = \left[\tilde{f}^{1/2}_{\mathbf{a}',\mathbf{a}}\cos\frac{\theta_j}{2} - \tilde{f}^{1/2}_{\mathbf{b}',\mathbf{b}}\sin\frac{\theta_j}{2}\right]^2, \tag{41}$$

$$\tilde{f}^{(j)}_{+} = \left[\tilde{f}^{1/2}_{\mathbf{a}',\mathbf{a}}\sin\frac{\theta_j}{2} + \tilde{f}^{1/2}_{\mathbf{b}',\mathbf{b}}\cos\frac{\theta_j}{2}\right]^2, \tag{42}$$

with

$$\tan\theta_j = \frac{4E^{1/2}_{\mathbf{a}',\mathbf{a}}E^{1/2}_{\mathbf{b}',\mathbf{b}}|\overline{\mathcal{B}}^{(j)}_{\mathbf{a},\mathbf{a}';\mathbf{b},\mathbf{b}'}|}{(\tilde{E}^{(j)}_{\mathbf{b}',\mathbf{b}})^2 - (\tilde{E}^{(j)}_{\mathbf{a}',\mathbf{a}})^2}, \tag{43}$$

where $\tilde{f}_{\mathbf{c}',\mathbf{c}} = f_{\mathbf{c}',\mathbf{c}}n_{\mathbf{c},\mathbf{c}'}$, $f_{\mathbf{c}',\mathbf{c}} = (2m_0/\hbar^2)E_{\mathbf{c}',\mathbf{c}}|z_{\mathbf{c},\mathbf{c}'}|^2$ is the oscillator strength corresponding to the $\mathbf{c}'\rightarrow\mathbf{c}$ transitions in the absence of the DE, and m_0 is the free electron mass. As was shown in Ref. 29 the following sum rule $\Sigma_{\mathbf{a}'}f_{\mathbf{a},\mathbf{a}'} = \langle\mathbf{a}|m_0/m^*|\mathbf{a}\rangle$ is fulfilled, where m^* is the spatially dependent effective mass.

In the above equations $\tan\theta_j$ represents the intermode coupling, with $\tan\theta_j=0$ stands for no coupling ($\overline{\mathcal{B}}^{(j)}_{\mathbf{a},\mathbf{a}';\mathbf{b},\mathbf{b}'}=0$), i.e., the diagonal approximation. Equations (41) and (42) let us write the MOS sum rule as

$$\tilde{f}^{(j)}_{-} + \tilde{f}^{(j)}_{+} = \tilde{f}_{\mathbf{a}',\mathbf{a}} + \tilde{f}_{\mathbf{b}',\mathbf{b}}, \tag{44}$$

which tells us that the sum of the modified oscillator strengths is independent of the intermode coupling: if due to the coupling $\tilde{f}^{(j)}_{-}$ increases then $\tilde{f}^{(j)}_{+}$ decreases accordingly, and vice versa.

From Eqs. (41) and (42) it is readily obtained that the relative height of the peaks is represented by the MOS ratio

$$\tilde{f}_{-}^{(j)}/\tilde{f}_{+}^{(j)} = \left(\tan\frac{\theta_j - \theta_j^{(0)}}{2}\right)^2, \tag{45}$$

where $[\tan(\theta_j^{(0)}/2)]^2 = \tilde{f}_{\mathbf{a}',\mathbf{a}}^{(j)}/\tilde{f}_{\mathbf{b}'\mathbf{b}}^{(j)}$. Note that $\theta_j^{(0)} = \pi/2$ for $\tilde{f}_{\mathbf{a}',\mathbf{a}} = \tilde{f}_{\mathbf{b}',\mathbf{b}}$. The case $\theta_j = 0$ corresponds to the absence of the intermode interaction (the diagonal approximation), i.e., $\tilde{f}_{-}/\tilde{f}_{+} \equiv \tilde{f}_{\mathbf{a}',\mathbf{a}}/\tilde{f}_{\mathbf{b}',\mathbf{b}}$. One can see that the MOS ratio $\tilde{f}_{-}^{(j)}/\tilde{f}_{+}^{(j)}$ is an even function of $\theta_j - \theta_j^{(0)}$ with its minimum zero value at $\theta_j = \theta_j^{(0)}$. Thus, with increasing intermode coupling, which corresponds to increasing θ_j from zero to $\theta_j^{(0)}$, the height of the low-energy peak decreases and vanishes (i.e., $\tilde{f}_{-}^{(j)} \equiv 0$) at $\theta_j = \theta_j^{(0)}$. This vanishing of the low-energy peak means that due to the intermode coupling all the energy of the collective excitations in the system is concentrated in the high-energy modified mode. For $\tilde{f}_{\mathbf{a}',\mathbf{a}} = \tilde{f}_{\mathbf{b}',\mathbf{b}}$ the low-energy peak never vanishes to zero since $\theta_j^{(0)} = \pi/2$ requires $|\overline{\mathcal{B}}_{\mathbf{a},\mathbf{a}';\mathbf{b},\mathbf{b}'}^{(j)}| \to \infty$, according to Eq. (43). For $\tilde{f}_{\mathbf{a}',\mathbf{a}}^{(j)} \neq \tilde{f}_{\mathbf{b}',\mathbf{b}}^{(j)}$ there is the finite value, $|\overline{\mathcal{B}}_{\mathbf{a},\mathbf{a}';\mathbf{b},\mathbf{b}'}^{(j)}| = |\overline{\mathcal{B}}_{\mathbf{a},\mathbf{a}';\mathbf{b},\mathbf{b}'}^{(j)}|_0$, that corresponds to strong intermode coupling, at which the low-energy peak vanishes to zero. According to the MOS sum rule, the height of the high-energy peak increases with growing intermode coupling for $\theta_j < \theta_j^{(0)}$. We should note that this prediction of the peak height behavior is confirmed with high accuracy by our numerical simulations of Eq. (35).

Within the MOS approach the relationship for the complex polarizability of the four-state system, with the broadening being incorporated, is reasonably presented in the following simple form:

$$\alpha_{jj}(\omega) = \frac{e^2\hbar^2}{m_0}\left[\frac{\tilde{f}_{-}^{(j)}}{(\hbar\omega_{-}^{(j)})^2 - (\hbar\omega)^2 - i2\hbar\omega\Gamma} + \frac{\tilde{f}_{+}^{(j)}}{(\hbar\omega_{+}^{(j)})^2 - (\hbar\omega)^2 - i2\hbar\omega\Gamma}\right]. \tag{46}$$

It should be emphasized that the parameter which determines the applicability and accuracy of the MOS approach for the systems of interacting modes is the ratio of Γ and the characteristic interlevel spacing of the system, i.e., $\gamma_{\mathrm{MOS}} = 2\Gamma/E_{\mathbf{c}',\mathbf{c}}$.

Note that Eq. (46) exactly describes the systems of noninteracting modes [the diagonal approximation, see Eq. (30)], when the height of the peak (more precisely the area under the peak) is proportional to $\tilde{f}_{\mathbf{a}',\mathbf{a}}$, which is treated as the MOS associated with the *a* mode of the collective excitations.

Note also that the expressions analogous to the above ones were derived in our previous paper[28] where the intersubband collective modes were considered in quantum well with two lowest subbands $n=1$ and $n=2$ occupied. There the collective modes were associated with $1 \to 2$ and $2 \to 3$ intersubband transitions. However, in contrast to the SQD, the intermode coupling in QWs can have resonant character only when appropriate conditions are met.[28,30]

4. Dipole-dipole interaction approximation

It is really worth mentioning a special and important approach to investigating the interdot dynamic *e-e* interaction in the QD systems. It is the dipole-dipole interaction approximation (DDA). Within the DDA the QDs of the lattice are treated as point dipoles which interact with each other. Note that the DDA is based on the assumption that the total field affecting the electrons in a QD can be assumed to be a uniform field in the volume of the QD.

Here we are going to exploit the DDA for the cases of QD systems when QDs are populated by many electrons and, especially, a few different types of the interstate electron transitions are allowed. To our best knowledge such cases have not been rigorously investigated taking into account the mode mixing and electron self-interaction.

Developing as in Ref. 31 we obtain the following elegant relation between the polarizability $\alpha(\omega)$ of an isolated single QD and the (effective) polarizability $\alpha_{jj}(\omega)$ of the QD located in a system of QDs:

$$\alpha_{jj}(\omega) = \frac{\alpha(\omega)}{1 - S^{(j)}\alpha(\omega)}. \tag{47}$$

The configuration parameter $S^{(j)}$, appearing in the above equation, represents the summation over the QDs to get the field at a given QD created by all the rest dipoles of the system [see Eq. (1.4) in Ref. 31]. For the considered here infinite 2D square lattice $S^{(j)} = \xi^{(j)}/d^3$ and $\xi^{(1)} = \xi^{(2)} = -\xi_0/2$, $\xi^{(3)} = \xi_0$, with $\xi_0 = -\Sigma'^{\infty}_{k,l=-\infty}(k^2+l^2)^{-3/2} \cong -9.0336$ (the term with $k=l=0$ is excluded in the summation).

It should be emphasized that Eq. (47) is general and can be applied for a variety of QD systems. Another advantage of Eq. (47) is its independence of the kind of QDs in the systems. All the information about the electronic structure of the dot and particular intradot *e-e* interactions is sacrificed in $\alpha(\omega)$, which is calculated by Eqs. (30) and (35) when $\overline{\mathcal{B}}_{\mathbf{a},\mathbf{a}';\mathbf{c},\mathbf{c}'}^{(j)} = \overline{L}_{\mathbf{a},\mathbf{a}';\mathbf{c},\mathbf{c}'}$ and the polarization index j is omitted. Using these expressions for $\alpha(\omega)$ we can obtain by means of Eq. (47) the relationships for $\overline{\mathcal{B}}_{\mathbf{a},\mathbf{a}';\mathbf{c},\mathbf{c}'}^{(j)}$ for QD systems within the DDA.

When the QD is considered as a two-state electron system (the diagonal approximation) the application of Eq. (47) results in Eqs. (30)–(33) with

$$\overline{\mathcal{B}}_{\mathbf{c},\mathbf{c}';\mathbf{c},\mathbf{c}'}^{(j)} = \overline{L}_{\mathbf{c},\mathbf{c}';\mathbf{c},\mathbf{c}'} - |\mu_{\mathbf{c},\mathbf{c}'}|^2 n_{\mathbf{c},\mathbf{c}'} S^{(j)}. \tag{48}$$

For the four-state system, (47) results in Eqs. (35)–(38) with, in addition to Eq. (48), the following relation takes place:

$$\overline{\mathcal{B}}_{\mathbf{a},\mathbf{a}';\mathbf{b},\mathbf{b}'}^{(j)} = \overline{L}_{\mathbf{a},\mathbf{a}';\mathbf{b},\mathbf{b}'} - |\mu_{\mathbf{a},\mathbf{a}'}\mu_{\mathbf{b},\mathbf{b}'}|\sqrt{n_{\mathbf{a},\mathbf{a}'} n_{\mathbf{b},\mathbf{b}'}}\, S^{(j)}. \tag{49}$$

The amazingly simple relationships (48) and (49) are very easy to exploit and allow us to make important conclusions. (i) In the DDA the interdot *e-e* interaction is controlled by the *bare* dipoles $\mu_{\mathbf{a},\mathbf{a}'}$ and $\mu_{\mathbf{b},\mathbf{b}'}$ (independently of the strength of intermode mixing), by the number of the electrons in the dots, and by the configuration of the QD system (i.e., dimension, size, and order). (ii) Within the DDA the

effects associated with intradot and interdot *e-e* interactions can be analyzed completely separately. In addition, assuming (i) and (ii) to be valid, the above relationships can be applied to other systems of identical QDs, and, moreover, even to systems of nonidentical QDs, provided the bare dipoles and the number of the electrons are known for each dot. In the next section the validity of the DDA is checked by comparison of the numerical results for the DE shift calculated with the help of Eqs. (48) and (49), and with the help of $\overline{\beta}^{(j)}_{\mathbf{a},\mathbf{a}';\mathbf{c},\mathbf{c}'}$.

III. NUMERICAL RESULTS AND DISCUSSION

In this section we discuss in detail the results of numerical calculations. Numerical calculations for $\overline{\beta}^{(j)}_{\mathbf{a},\mathbf{a}';\mathbf{c},\mathbf{c}'}$ have been performed for systems of SQDs with infinite and finite potential barrier. Both the two-state and four-state systems are investigated. However, the effective polarizability is considered only for the lattice of SQDs with finite potential barrier and we restrict it to the four-state system since it reveals much more interesting features of the DE than the two-state model.

We consider a square lattice ($d_1=d_2=d$) of identical GaAs SQDs in $Al_{0.3}Ga_{0.7}As$ medium. The parameters used are: the offset of the potential well is $U_0=227.9$ meV, the electron effective masses in the dot and barrier are $m_d=0.066m_0$ and $m_b=0.092m_0$, respectively. $\Gamma=1$ meV and $\epsilon=13.18$. As has been mentioned, the difference between the dielectric constants of the dot and barrier materials is neglected. We assume that each dot contains a fixed number of electrons: $N_{\mathrm{QD}}=8$ [2 at the lowest level (1, 0, 0) and 6 at the next level $(1,1,m)$] for the four-state system, and $N_{\mathrm{QD}}=2$ [at (1,0,0)] for the two-state system.

For the four-state system the dot radius $R=95$ Å is chosen so that the dot contains only one more vacant energy level [states $(1,2,m)$] in addition to the two occupied levels. Note that this situation is far from the infinite deep SQDs case. Self-consistent solution of Eq. (7) gives $E_{1,0}=-91$ meV, $E_{1,1}=-55.4$ meV, and $E_{1,2}=-10.7$ meV. For comparison, when the static intradot *e-e* interaction is neglected $E_{1,0}=-184.2$ meV, $E_{1,1}=-138.3$ meV, and $E_{1,2}=-82.3$ meV. Thus, the direct Coulomb interaction reduces the energy separation between states $(1,2,m)$ and $(1,1,m)$ from 56 to 44.7 meV.

It should be noted that the exchange-correlation interaction reduces the effect of the direct Coulomb interaction so that the bound levels in the dot drop down by about 30 meV (see Fig. 1 in Ref. 26). However, the interlevel gap changes by nearly 2 meV. The effect of the exchange-correlation interaction also means that the considered three-bound level SQDs can be realized at a considerably smaller radius. A special case should be mentioned when one of the levels involved in the transitions is located very close to the QD top. Then the exchange-correlation effect can be substantial.

Numerical simulations show that the electron tunnelling between the dots (with $R=95$ Å) can be practically ignored for $d>400$ Å. For the four-state system the following dipole transitions are considered: $\mathbf{a}\leftrightarrows\mathbf{a}'$ and $\mathbf{b}\leftrightarrows\mathbf{b}'$, with $n_{\mathbf{a},\mathbf{a}'}=2$ and $n_{\mathbf{b},\mathbf{b}'}=4$.

For comparison we consider also the two-state system with transitions $(1,0,0)\leftrightarrows(1,1,0)$ only. The notations used are $\mathbf{g}=(1,0,0)$ and $\mathbf{g}'=(1,1,0)$ with $n_{\mathbf{g},\mathbf{g}'}=2$.

Note that for the infinitely deep SQD with one electron the dipole matrix element takes a very simple form, useful for approximate evaluation for other SQDs, as

$$|z_{\mathbf{c},\mathbf{c}'}| = RM_{\mathbf{c},\mathbf{c}'}, \tag{50}$$

where $M_{(1,0,0)(1,1,0)}=0.306$, $M_{(1,1,0)(1,2,0)}=0.315$, $M_{(1,1,\pm1)(1,2,\pm1)}=0.273$. Then $f_{(1,1,0)(1,2,0)}/f_{(1,1,\pm1)(1,2,\pm1)}=1.331$.

To calculate the depolarization shifted transition energy for the 2DRLSQD it is most convenient to utilize the Cartesian coordinate system (x,y,z) with axis orientation depending on the polarization of the light. Namely, for the normal ("$\perp$") incident light polarization ($j=3$): $x=x_1$, $y=x_2$, and $z=x_3$. For the in-plane incident light polarization with $j=1$: $x=x_2$, $y=x_3$, $z=x_1$; and with $j=2$: $x=x_3$, $y=x_1$, $z=x_2$. (For square 2DRLSQDs these two polarizations are equivalent and will be labeled by "$\parallel$.")

We compare our numerical results with those obtained within the modified oscillator strength approach [see Eq. (46)] and the DDA [see Eqs. (48) and (49)]. We would like to note that the numerical calculations require high accuracy and are very time consuming especially for $d/2R>5$. To make conclusions about accuracy when comparing the data presented in the figures one should keep in mind that different computer codes are used for calculation of $\beta^{\perp}(\mathbf{a},\mathbf{a}';\mathbf{c},\mathbf{c}')$, $\beta^{\parallel}(\mathbf{a},\mathbf{a}';\mathbf{c},\mathbf{c}')$, and $L(\mathbf{a},\mathbf{a}';\mathbf{c},\mathbf{c}')$. In addition, any value of $\beta^{(j)}(\mathbf{a},\mathbf{a}';\mathbf{c},\mathbf{c}')$ is a sum of a great deal (more than 100 for $d/2R>2$) of the terms [see Eq. (26)] calculated for different m_1 and m_2, and the accuracy of the calculations depends on the value of $m_{1(2)}R/d$. This makes the calculated data in the figures look similar to "experimental" data, because no two values in the figures are calculated with exactly the same accuracy. Note that the simplicity of the DDA becomes very attractive in the above context.

A. Lattice of SQDs with one electron per dot

It is very convenient and instructive to consider first a lattice of SQDs with one electron per dot. As there is no intradot *e-e* interaction in such a lattice the DE is formed due to the interdot *e-e* interaction. Let us make the basic properties of the DE in the lattice clear.

Figures 1 and 2 present the numerical results obtained by Eq. (28) as well as the data obtained within the DDA. To truly estimate the accuracy, note that these figures are reduced from source figures, which look similar to Figs. 4(d) and 5(d), by setting the intradot effect to zero as it is the pure self-interaction. For comparison the correction to the interlevel gap caused by the static interdot *e-e* interaction (see Fig. 8) is shown in Fig. 1 too.

From Figs. 1 and 2 one can conclude the following.

(i) The DDA represents the DE shift caused by dynamic interdot *e-e* interaction very well for both the infinite and finite deep SQDs with one electron per dot for transitions $\mathbf{g}\rightleftarrows\mathbf{g}'$ even when interdot separation is comparable with $2R$ (which means practically at any $d/2R$).

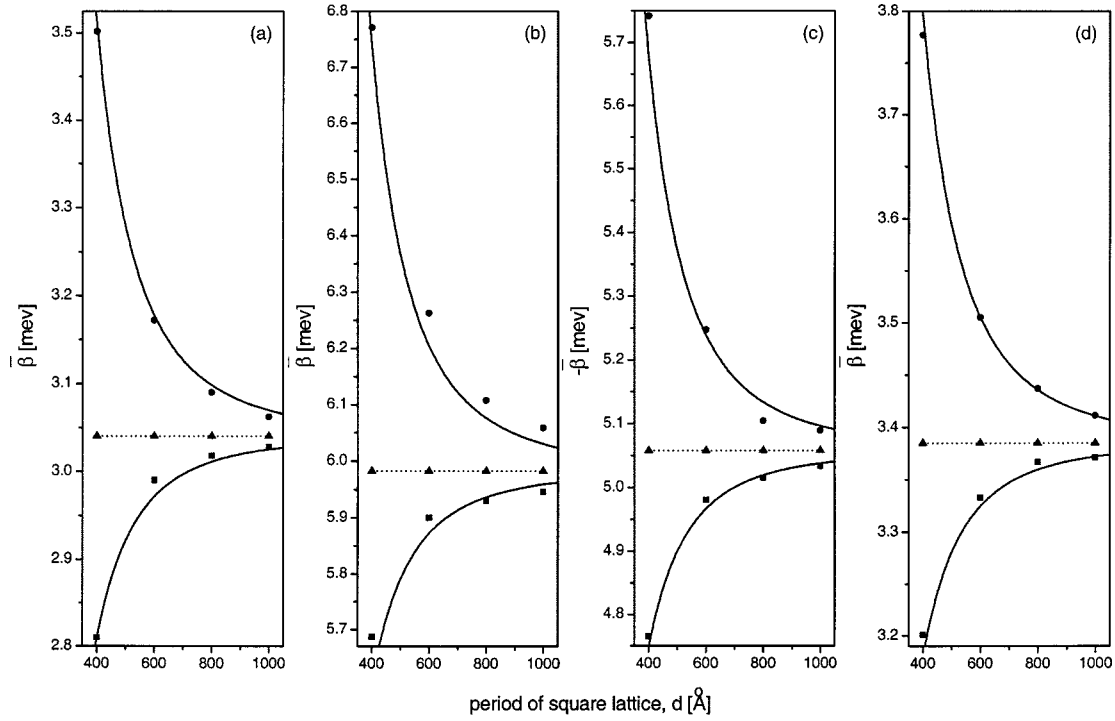

FIG. 4. Dependence of $\overline{\beta}^{(j)}_{\mathbf{a},\mathbf{a}';\mathbf{a},\mathbf{a}'}$ (a), $\overline{\beta}^{(j)}_{\mathbf{b},\mathbf{b}';\mathbf{b},\mathbf{b}'}$ (b), $-\overline{\beta}^{(j)}_{\mathbf{a},\mathbf{a}';\mathbf{b},\mathbf{b}'}$ (c), and $\overline{\beta}^{(j)}_{\mathbf{g},\mathbf{g}';\mathbf{g},\mathbf{g}'}$ (d) for normal (circle symbols) and in-plane (square symbols) incident light polarizations upon the interdot distance in a square lattice of finite deep SQDs at $R=95$ Å. $n_{\mathbf{a},\mathbf{a}'}=2$, $n_{\mathbf{a},\mathbf{b}'}=4$, and $n_{\mathbf{g},\mathbf{g}'}=2$. The intradot dynamic *e-e* interaction is represented by the dot lines with triangular symbols. The solid lines represent the DDA.

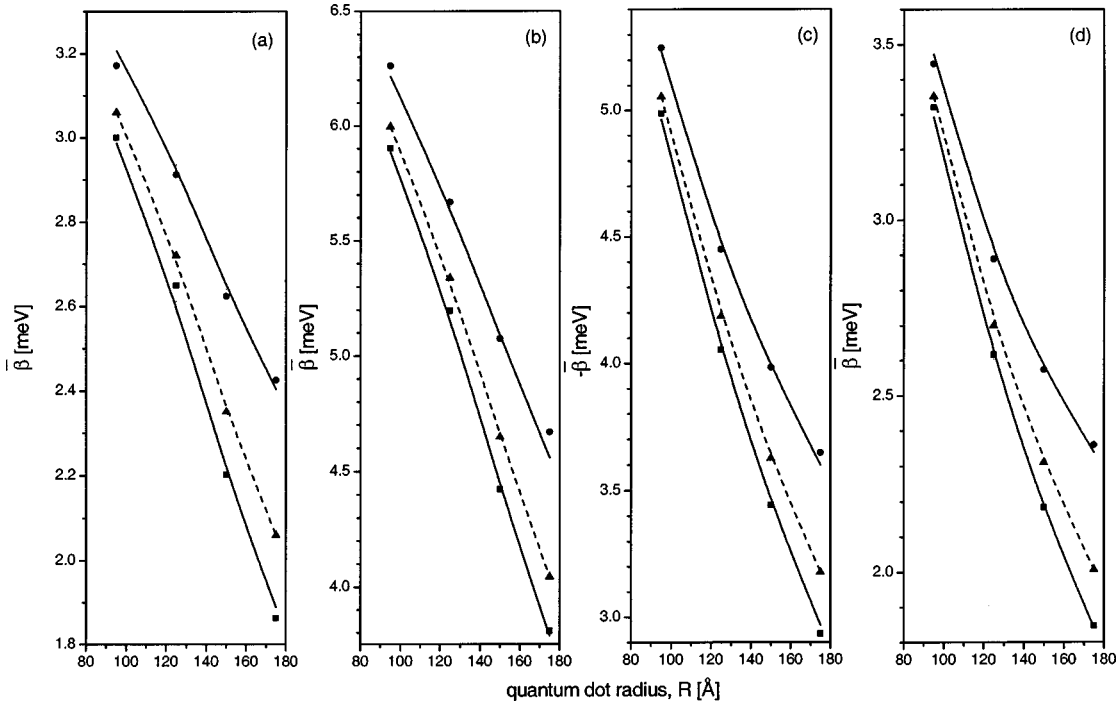

FIG. 5. Dependence of $\overline{\beta}^{(j)}_{\mathbf{a},\mathbf{a}';\mathbf{a},\mathbf{a}'}$ (a), $\overline{\beta}^{(j)}_{\mathbf{b},\mathbf{b}';\mathbf{b},\mathbf{b}'}$ (b), $-\overline{\beta}^{(j)}_{\mathbf{a},\mathbf{a}';\mathbf{b},\mathbf{b}'}$ (c), and $\overline{\beta}^{(j)}_{\mathbf{g},\mathbf{g}';\mathbf{g},\mathbf{g}'}$ (d) for normal (circle symbols) and in-plane (square symbols) incident light polarizations upon the radius of finite deep SQDs at $d=600$ Å. $n_{\mathbf{a},\mathbf{a}'}=2$, $n_{\mathbf{b},\mathbf{b}'}=4$, and $n_{\mathbf{g},\mathbf{g}'}=2$. Intradot dynamic *e-e* interaction is represented by the dot lines with triangular symbols. The solid lines represent the DDA.

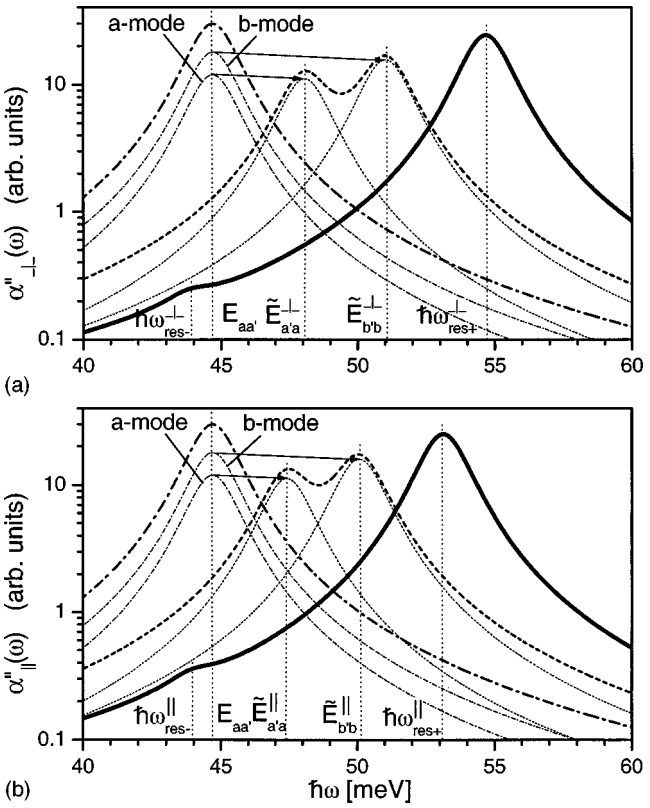

FIG. 6. Dependence of $\alpha''_{\perp}(\omega)$ (a) and $\alpha''_{\parallel}(\omega)$ (b) upon photon energy of incident radiation for square lattice of finite deep SQDs described in the text. $R=95$ Å and $d=400$ Å. $n_{\mathbf{a},\mathbf{a}'}=2$ and $n_{\mathbf{b},\mathbf{b}'}=4$. The solid line represents results obtained including intermode coupling into the dynamic *e*-*e* interaction. Dash lines correspond to the diagonal approximation (i.e., no intermode coupling). Dash-dotted lines are obtained neglecting dynamic Coulomb interaction. In the two last approximations the separate contributions associated with *a*-mode and *b*-mode to $\alpha''_{\perp}(\omega)$ and $\alpha''_{\parallel}(\omega)$ are also presented by thin lines.

(ii) A decrease of the confining potential causes an increase of the absolute value of the DE shift because of the increase of the dipole matrix elements through modification of the electron wave functions and their extent beyond the QD boundary.

(iii) An infinite deep QD approximation results in an essential underestimation of the DE shift.

(iv) The DE shift induced by the interdot interaction, practically vanishes for $d/2R>5$.

(v) An increase of the dipole matrix elements with growing QD size is responsible for the increase of the absolute value of the DE shift associated with the interdot *e*-*e* interaction.

(vi) At a fixed electron sheet density (when $d=$const) the DE shift changes just because of the change of the QD size.

One can see that for spherical QDs the exponential factor (see Sec. II A 2) does not manifest itself. Note the increase of the dipole matrix elements $|z_{\mathbf{c},\mathbf{c}'}|$ with decreasing potential barrier [against the values by Eq. (50) in the brackets] at $R=95$ Å: $|z_{(1,0,0)(1,1,0)}|=36.2$ Å (29.1 Å), $|z_{(1,1,0)(1,2,0)}|=40.1$ Å (29.9 Å), and $|z_{(1,1,\pm1)(1,2,\pm1)}|=34.7$ Å (25.9 Å). The value of $M_{\mathbf{c},\mathbf{c}'}$ in Eq. (50) decreases with growing R, especially at 95 Å$<R<$150 Å up to 10%.

B. Lattice of infinitely deep SQDs

It is also convenient is to discuss features of $\overline{\beta}^{(j)}_{\mathbf{a},\mathbf{a}';\mathbf{c},\mathbf{c}'}$ for a square lattice of infinite deep SQDs assuming for simplicity $V_{sc}(r)=0$. (Then the one-electron wave functions can be written in terms of the Bessel functions.) The advantage of such a simplified model is that $\tilde{\beta}^{(j)}_{\mathbf{a},\mathbf{a}';\mathbf{c},\mathbf{c}'}$ in Eq. (29) then depends only upon ratio $d/2R$, which means that $(\overline{\beta}^{(j)}_{\mathbf{a},\mathbf{a}';\mathbf{c},\mathbf{c}'}d)$ is common for any square lattice of infinitely deep SQDs with the one-electron wave functions. Thus, having $(\overline{\beta}^{(j)}_{\mathbf{a},\mathbf{a}';\mathbf{c},\mathbf{c}'}d)$ calculated we can get $\overline{\beta}^{(j)}_{\mathbf{a},\mathbf{a}';\mathbf{c},\mathbf{c}'}$ for any lattice period d and dot radius R. Further we use label $\overline{\beta}^{(j)}$ (and $\overline{\beta}$) when speaking about $\overline{\beta}^{(j)}_{\mathbf{a},\mathbf{a}';\mathbf{a},\mathbf{a}'}$, $\overline{\beta}^{(j)}_{\mathbf{b},\mathbf{b}';\mathbf{b},\mathbf{b}'}$, $\overline{\beta}^{(j)}_{\mathbf{a},\mathbf{a}';\mathbf{b},\mathbf{b}'}$, and $\overline{\beta}^{(j)}_{\mathbf{g},\mathbf{g}';\mathbf{g},\mathbf{g}'}$ independently of specific transitions (and light polarization).

In addition to $(\overline{\beta}^{(j)}_{\mathbf{a},\mathbf{a}';\mathbf{c},\mathbf{c}'}d)$, the values of $(\overline{L}_{\mathbf{a},\mathbf{a}';\mathbf{c},\mathbf{c}'}R)$ are also independent of R and common for all single SQDs. Then having $\overline{\beta}^{(j)}_{\mathbf{a},\mathbf{a}';\mathbf{c},\mathbf{c}'}$ and $\overline{L}_{\mathbf{a},\mathbf{a}';\mathbf{c},\mathbf{c}'}$ it is easy to separate the DE shift associated with the interdot and intradot dynamic *e*-*e* interactions.

To illustrate the strength of the interdot *e*-*e* interaction in the system with one electron per dot, we present in Figs. 3(a)–3(d) the variation of $(\overline{\beta}^{(j)}_{\mathbf{a},\mathbf{a}';\mathbf{c},\mathbf{c}'}d)$ as a function of $d/2R$. For $n_{\mathbf{a}}$, $n_{\mathbf{c}}$ electrons per QD at states **a** and **c**, respectively, the values in Figs. 3(a)–3(d) should be multiplied by $\sqrt{n_{\mathbf{a}}n_{\mathbf{c}}}$.

From Figs. 3(a)–3(d) one can conclude that the DDA represents the contribution of the dynamic interdot *e*-*e* interaction in the DE shift well for any type of electron transition and any $d/2R$ for the Bessel wave functions. Figures 3(a)–3(d) show also that the values of $\overline{\beta}$ for different transitions can differ considerably.

To exploit the great advantage of the applicability of the DDA for the case of many electrons per dot one should know the values of $L_{\mathbf{a},\mathbf{a}';\mathbf{c},\mathbf{c}'}$. The numerical values of $(L_{\mathbf{a},\mathbf{a}';\mathbf{c},\mathbf{c}'}R)$ are as follows: $L_{\mathbf{a},\mathbf{a}';\mathbf{a},\mathbf{a}'}R=405.0$ meV Å, $L_{\mathbf{b},\mathbf{b}';\mathbf{b},\mathbf{b}'}R=265.7$ meV Å, $L_{\mathbf{a},\mathbf{a}';\mathbf{b},\mathbf{b}'}R=-223.8$ meV Å, $L_{\mathbf{g},\mathbf{g}';\mathbf{g},\mathbf{g}'}R=392.3$ meV Å. To obtain $(\overline{L}_{\mathbf{a},\mathbf{a}';\mathbf{c},\mathbf{c}'}R)$ for $n_{\mathbf{a}}$ and $n_{\mathbf{c}}$ electrons at the levels **a** and **c**, respectively, these values should be multiplied by $(\sqrt{n_{\mathbf{a}}n_{\mathbf{c}}}-\delta_{\mathbf{a},\mathbf{c}})$. Note that for more than one electron in a single SQD the DE shift due to the intradot *e*-*e* interaction decreases with growing QD size. This is associated with decrease of the *e*-*e* interaction potential in a bigger restricting room.

We want to emphasize that the numerical values (for $1<d/2R<5$) obtained above are common for any infinitely deep SQD with one-electron wave functions, which are either single dots or form the square lattice. A change of the dielectric constant changes the values according to Eqs. (15) and (29). In part it moves all of the lines in Fig. 3 up or down on the scale. These values are very useful for an instant approximate estimation even for SQDs with finite barrier and many electrons.

C. Lattice of SQDs with finite potential barrier

Wave functions of electrons are modified by a finite potential barrier of the quantum dot and, in addition, by the

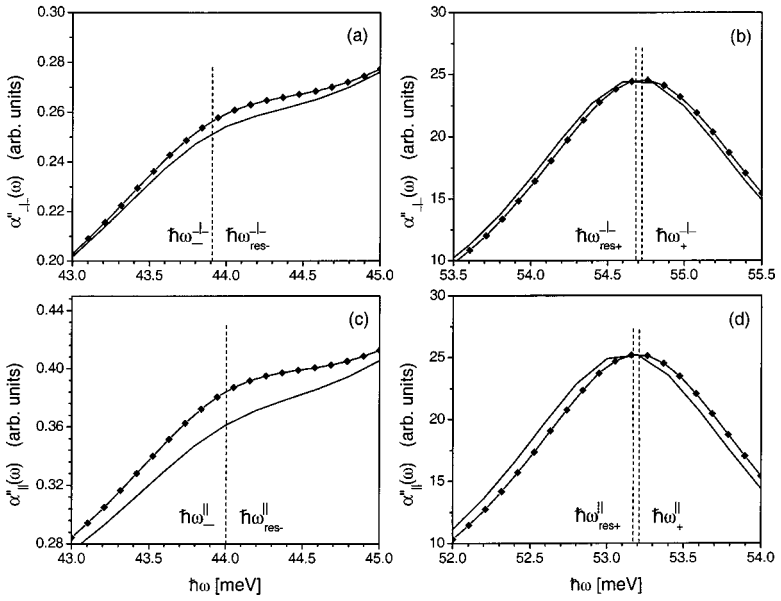

FIG. 7. Near-peak absorption spectra of the four-state system including the intermode coupling predicted by the MOS approach (solid lines with diamonds) are compared with the corresponding exact spectra (solid lines) represented by solid lines in Fig. 6. The position of the peaks is marked by the vertical dash line.

static *e-e* interaction (see further). The dot radius becomes an important parameter for this effect. As a result, $\tilde{\beta}^{(j)}_{\mathbf{a},\mathbf{a}';\mathbf{c},\mathbf{c}'}$ in Eq. (29) is a function not of the ratio $d/2R$ but of R and d independently, and, thus, values of $\overline{\beta}^{(j)}_{\mathbf{a},\mathbf{a}';\mathbf{c},\mathbf{c}'}$ are specific for each system.

Figures 4 and 5 present the DE shift in the lattice of SQDs for two-state ($N_{\mathrm{QD}}=2$) and four-state ($N_{\mathrm{QD}}=8$) systems. These figures demonstrate all the features of the DE shift disclosed in the two previous subsections. It is worth emphasizing that in Figs. 4–6 both the interdot and intradot *e-e* interaction work together.

First of all, Figs. 4 and 5 confirm that the DDA represents the DE shift well due to the dynamic interdot *e-e* interaction for the square lattice of the finite deep SQDs for any type of electron transitions and practically any $d/2R$. Note that the match with the DDA in the figures (as well as in Figs. 1–3) can be treated as excellent if the accuracy for the calculated $\overline{\beta}$ and $\overline{L}_{\mathbf{a},\mathbf{a}';\mathbf{c},\mathbf{c}'}$ is adopted to be within 0.5%.

Figure 5 gives a good illustration of the opposite effect of change of the QD size upon the influence of the interdot and intradot dynamic *e-e* interaction on the DE. Note that the contribution of the interdot interaction to the DE shift is the difference between $\overline{\beta}^{(j)}_{\mathbf{a},\mathbf{a}';\mathbf{c},\mathbf{c}'}$ and $\overline{L}_{\mathbf{a},\mathbf{a}';\mathbf{c},\mathbf{c}'}$, which is represented within the DDA as the difference between the solid and dot lines in Fig. 5.

With growing R the absolute value of the DE shift increases (decreases) for the interdot (intradot) interaction, and the shift due to the interdot interaction is more sensitive to the R change. It is important to note that the relative contribution of the interdot and intradot *e-e* interaction into the DE shift is determined by the size of the SQDs. (Note that, in general, in addition to the QD size, the QD shape can also affect the relative contribution.) Figure 5 also shows that it is the contribution of the intradot interaction that determines the overall value of the DE shift for our QD systems.

It is important to notice the reducing effect of the decrease of the confinement potential on the contribution to the DE shift caused by the intradot *e-e* interaction. As it is with the growing QD size the reason is the spreading out of the electron wave functions in the bigger space, which reduces the intradot *e-e* interaction. Note that the static intradot *e-e* interaction results in an additional extension of the wave functions. The values of $L_{\mathbf{a},\mathbf{a}';\mathbf{c},\mathbf{c}'}$ for the considered finite deep SQD (see Figs. 4 and 5) are about 30% less than those for the infinite deep SQD (see $L_{\mathbf{a},\mathbf{a}';\mathbf{c},\mathbf{c}'}R$ in Sec. III B).

It should be noted that for $R>100$ Å the interlevel spacing comes close to the energies of LO phonons in the system and a more careful analysis, including the coupling of the collective modes with the above phonons, is needed which is beyond the scope of this paper. According to our numerical calculations, the value of $\overline{\beta}$ for 2DRLSQD with $d_1 \neq d_2$ can be roughly taken as an average between $\overline{\beta}$ values for square lattices with lattice periods d_1 and d_2, if d_1 and d_2 are rather close to each other. However, when $\max(d_1,d_2)/\min(d_1,d_2)>2$ the DE shift in such a lattice appears to be smaller (in the absolute values) than that for the square lattice with the period being $\min(d_1,d_2)$.

Figure 6 displays absorption spectra [more exactly $\alpha''_{11}(\omega)=\alpha''_{22}(\omega)\equiv\alpha''_{\parallel}(\omega)$ and $\alpha''_{33}(\omega)\equiv\alpha''_{\perp}(\omega)$] for the normal and in-plane polarization of incident radiation at $d=400$ Å. The presented results illustrate the importance of the dynamic interdot interaction very well. This interaction causes the shift of the positions of two peaks in the absorption spectra to the energies $\hbar\omega^{\perp}_{\mathrm{res}-}$, $\hbar\omega^{\perp}_{\mathrm{res}+}$ and $\hbar\omega^{\parallel}_{\mathrm{res}-}$, $\hbar\omega^{\parallel}_{\mathrm{res}+}$. The positions of the high-energy peaks are determined from the spectrum (see also Fig. 7) to be $\hbar\omega^{\perp}_{\mathrm{res}+}=54.69$ meV and $\hbar\omega^{\parallel}_{\mathrm{res}+}=53.15$ meV. The positions of the low-energy peaks are hard to determine from the spectra. That is why we take them as close to the calculated values $\hbar\omega^{\perp}_{-}$ and $\hbar\omega^{\parallel}_{-}$: $\hbar\omega^{\perp}_{\mathrm{res}-}\approx\hbar\omega^{\perp}_{-}=43.9$ meV and $\hbar\omega^{\parallel}_{\mathrm{res}-}\approx\hbar\omega^{\parallel}_{-}=44$ meV.

Figure 6 also shows the substantial influence of the intermode coupling on the absorption spectra. Due to the near resonant character of this coupling considerable splitting of

the peaks and considerable redistribution of the oscillator strength takes place. Note that observation of the double peak structure in the absorption spectra is possible when the broadening energy Γ is sufficiently small. For bigger Γ the two peaks on the spectra cannot be distinguished: the lower-energy peak practically vanishes. However, the position of the higher energy peak can be correctly determined only by taking into account the intermode interaction. It should be emphasized that all six electrons at the second level $(1,1,m)$ contribute to the depolarization shift.

A simulation shows that even in the absence of the mode coupling (the diagonal approximation) the resonant energies deviate from the level separation. For example, taking $d=400$ Å we get $\widetilde{E}^{(1)}_{\mathbf{a}',\mathbf{a}}=\widetilde{E}^{(2)}_{\mathbf{a}',\mathbf{a}}=\widetilde{E}^{\parallel}_{\mathbf{a}',\mathbf{a}}=47.4$ meV and $\widetilde{E}^{(1)}_{\mathbf{b}',\mathbf{b}}=\widetilde{E}^{(2)}_{\mathbf{b}',\mathbf{b}}=\widetilde{E}^{\parallel}_{\mathbf{b}',\mathbf{b}}=50.2$ meV, $\widetilde{E}^{(3)}_{\mathbf{a}',\mathbf{a}}=\widetilde{E}^{\perp}_{\mathbf{a}',\mathbf{a}}=51.1$ meV and $\widetilde{E}^{(1)}_{\mathbf{b}',\mathbf{b}}=\widetilde{E}^{(\perp)}_{\mathbf{b}',\mathbf{b}}=48.1$ meV. Note, that although the depolarization shift is substantial the difference $|\widetilde{E}^{(j)}_{\mathbf{a}',\mathbf{a}}-\widetilde{E}^{(j)}_{\mathbf{b}',\mathbf{b}}|$ is small $(\ll\widetilde{E}^{(j)}_{\mathbf{a}',\mathbf{a}})$. The relative intensity of the *a* and *b* modes is described in the diagonal approximation by the ratio $\widetilde{f}_{\mathbf{a}',\mathbf{a}}/\widetilde{f}_{\mathbf{b}',\mathbf{b}}$ which takes the value $2/3$.

Figures 1–6 demonstrate a strong dependence of the DE upon the polarization of the incident light: the resonance photon energy for the normal light polarization is always bigger than that for the in-plane light polarization. It is important to note that in our approximations the difference between these resonance energies can be treated as independent of the static interdot interaction. In addition, our numerical calculations for the case of the in-plane polarization reveal different contributions to the DE from the lattice sites of different lattice rows. At $d=400$ Å, only the sites in the row perpendicular to the polarization direction contribute to the DE. At $d>500$ Å the situation changes: the dots in the row along the polarization direction make a major contribution to the DE. This again points to the importance of ratio $d/2R$ for the polarization dependence of the DE.

Figure 7 demonstrates that the approach of the modified oscillator strength excellently represents the absorption spectra of the considered four-state electron system. The positions of the peaks (more precisely the resonant energies) within the MOS approach are calculated by Eq. (38) as $\hbar\omega^{\perp}_{-}=43.9$ meV, $\hbar\omega^{\perp}_{+}=54.72$ meV, and $\hbar\omega^{\parallel}_{-}=44$ meV, $\hbar\omega^{\parallel}_{+}=53.2$. One can see in Figs. 7(b) and 7(d) that the error in the high-energy peak position (induced by the broadening) $|\hbar\omega^{(j)}_{+}-\hbar\omega^{(j)}_{\mathrm{res}+}|$ for $\Gamma=1$ meV is near 0.03 meV, that is, practically negligible. As Figs. 7(a) and 7(c) show the error of the position of the low-energy peaks is hard to determine. The height of the high-energy peaks is predicted very accurately $(<1\%)$ within the MOS approach for $\Gamma=1$ meV. The error for the low-energy peak height, being about 5%, is associated with the considerable contribution of the tail of the high-energy peak. Note that the MOS approach predicts very accurately not only the ratio of the height of the peaks, but also the absolute value of the peak height, especially the high-energy peak height. Our numerical simulations confirm with high accuracy the vanishing of the low-energy peaks at $|\overline{\mathcal{B}}^{\perp}_{\mathbf{a},\mathbf{a}';\mathbf{b},\mathbf{b}'}|_0=8.154$ meV and $|\overline{\mathcal{B}}^{\parallel}_{\mathbf{a},\mathbf{a}';\mathbf{b},\mathbf{b}'}|_0=7.488$ meV. Comparing these values with those of our system, $|\overline{\mathcal{B}}^{\perp}_{\mathbf{a},\mathbf{a}';\mathbf{b},\mathbf{b}'}|=5.742$ meV and $|\overline{\mathcal{B}}^{\parallel}_{\mathbf{a},\mathbf{a}';\mathbf{b},\mathbf{b}'}|=4.765$ meV, we can conclude that there is strong intermode coupling in the system. That is why the low-energy peak is so weak in the spectra.

As is mentioned in Sec. II B 3 the ratio γ_{MOS} determines the accuracy of the results obtained within the MOS approach. Our numerical simulations show that the MOS approach is very accurate at $\Gamma=3$ meV ($\gamma_{\mathrm{MOS}}=0.13$) in predicting the position and height of the high-energy peak. (The low-energy peak is not observed.) Even at $\Gamma=7$ meV ($\gamma_{\mathrm{MOS}}=0.31$) the error of the peak position is about 0.2 meV, while the error of the peak height is near 1%. Thus, we can conclude that the MOS approach excellently represents the multimode systems for reasonable values of Γ.

Above we have considered the effect of d on the DE at fixed N_{QD}. Now we discuss the influence of N_{QD} on the DE at fixed d. The DE is determined by values of $\overline{\beta}^{(j)}_{\mathbf{a},\mathbf{a}';\mathbf{a},\mathbf{a}'}$, $\overline{\beta}^{(j)}_{\mathbf{b},\mathbf{b}';\mathbf{b},\mathbf{b}'}$ and $\overline{\beta}^{(j)}_{\mathbf{a},\mathbf{a}';\mathbf{b},\mathbf{b}'}$. Calculations show that N_{QD} affects these values mainly directly by means of $n_{\mathbf{a},\mathbf{a}'}$ and $n_{\mathbf{b},\mathbf{b}'}$, while the influence of N_{QD} on values of $\beta(\mathbf{a},\mathbf{a}';\mathbf{c},\mathbf{c}')$ (through a change of parameters of the electron system in the dot) is weak. It should be emphasized that N_{QD} denotes the number of electrons *in* QDs, not in the whole structure. [Numerical results show that decrease of N_{QD} by 1 induces increase of $E_{\mathbf{a},\mathbf{a}'}$ by about 1–1.5 meV (while $E_{\mathbf{a}}$ decreases by about 10 meV for different levels), and the dipole matrix elements decrease by about 1.5%, i.e., are practically untouched.]

Finally, we want to emphasize that the analytical results and the majority of the obtained numerical results demonstrating new interesting and important features of the DE are valid for the systems of quantum dots of other shape. The specific spherical shape of dots utilized in this work makes some results (especially the intermode coupling) much more pronounced due to the resonance conditions for the interaction. Inspection shows that all these results are applied to ellipsoidal quantum dots with an eccentricity of up to 15%. In an ellipsoidal dots state $(1,l,0)$ is split off from states $(1,l,-1)$ and $(1,l,1)$ which are not split off from each other $(l=1,2)$. Rather a small eccentricity supports the resonance conditions.[10]

It should be noted that the presented numerical results describe rather small (95 Å) identical spherical quantum dots in an ideal square 2D lattice with rather small periods. Unfortunately, the currently manufactured quantum dots of such a size are not identical enough and are not organized into a regular lattice. This makes a direct quantitative comparison of our numerical results with the available experimental data difficult.

As it has been mentioned, measurements of the influence of interdot coupling on the interlevel resonance frequencies have been performed by Yakimov *et al.*[2] However, the authors investigated only a dense array of (disordered) *p*-type Ge/Si self-assembled anisotropic and inhomegeneously broadened quantum dots. Nevertheless, the results reported in the above paper show the considerable contribution of the interdot coupling to the DE. They observed, in particular, not

only a characteristic absorption peak shift but also a narrowing (induced by the DE) of the inhomogeneously broadened absorption line. This indicates that inhomogeneous broadening cannot be simply incorporated into the broadening parameter Γ.

IV. CONCLUSION

In conclusion, the depolarization effect on the interlevel response of the electron systems is investigated in detail for single SQDs as well as for two-dimensional square lattices of SQDs. It is established that photon absorption due to the dipole interlevel transitions in an individual SQD is considerably affected by the dynamic direct intradot *e-e* interaction. The linear optical response of dense packed 2D lattices of SQDs can be additionally affected by the DE associated with the dynamic direct interdot *e-e* interaction. The correct description of the above interaction should take into account so-called umklapp processes. It is established that the electron self-interaction is an unavoidable problem for the QD systems (especially with a relatively small number of electrons) and should be dealt with care when we work in the self-consistent field approach.

Values are found which can be used for a fast approximate estimation of the DE shift in *any* single SQD and 2D square lattice of SQDs. It was established that the dipole-dipole interaction approximation well represents the DE shift associated with the dynamic interdot *e-e* interaction for any type of electron transition, for practically any size parameters of the lattice, and for any potential barrier of the SQDs. In part, it was shown that in this approximation the effects associated with the intradot and interdot dynamic *e-e* interaction can be analyzed separately. The obtained results indicate also that the DE can cause not only the blueshift but also peak splitting (due to intermode coupling) when two lowest levels are occupied. The approach employing the concept of the modified oscillator strength is very useful for describing the effect associated with the above-mentioned intermode coupling.

Strong dependence of the DE upon the incident light polarization was demonstrated for the dense packed lattice. It was shown that the difference between the resonant photon energies for the normal and in-plane light polarization can be treated as independent of the static interdot interaction.

The three-dimensional nature of the QD systems was found to cause a number of effects. It was shown that ratio $d/2R$, the dot radius R, and the lattice period d can be used as driving parameters defining the features of the system response. It was shown that with growing dot radius the absolute value of the DE shift associated with the intradot (interdot) dynamic *e-e* interaction decreases (increases), so that R can determine the dominant contribution (of the intradot or interdot interaction) to the total shift.

It was also found that a decrease of potential barrier of quantum dots increases (decreases) the strength of the DE associated with the interdot (intradot) *e-e* interaction. The presented results disclose some important physical aspects of the electromagnetic response of QD lattices, in particular, strong dependence on the polarization of the incident radiation, effect of the size parameters (d and R) of the lattice, which can manifest themselves experimentally and be useful for application.

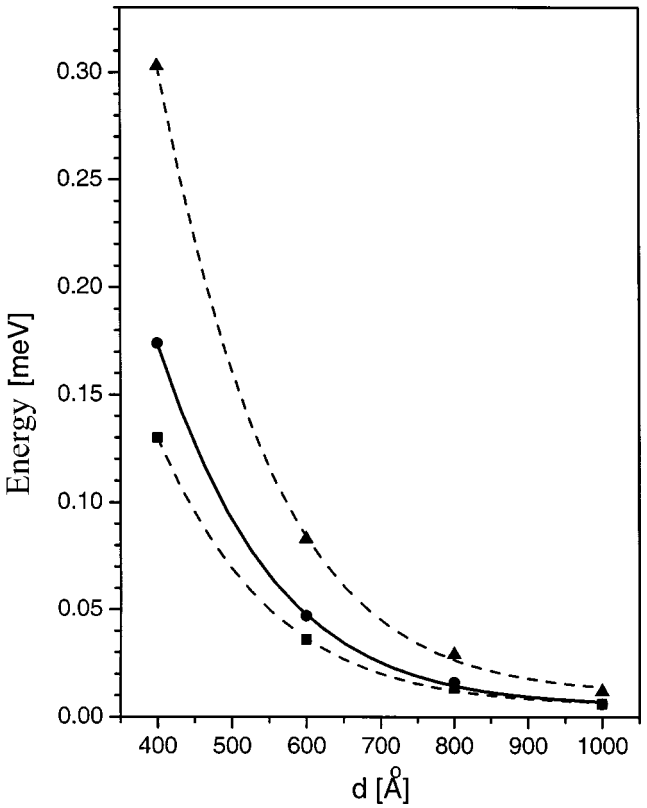

FIG. 8. Shift of the $E_{1,0}$ (square symbols) and $E_{1,1}$ (triangle symbols) energy, and modification of the gap between them $E_{1,1}-E_{1,0}$ (circle symbols) due to the static interdot *e-e* interaction as function of the interdot distance. $R=95$ Å. One electron is per QD.

ACKNOWLEDGMENTS

V.B. is grateful to P. Sokolowski for providing the opportunity to perform numerical calculations on the supercomputer grid of the Wayne State University. The work of M.Z. was partially supported by Grant No. PBZ-MIN-008/P03/2003.

APPENDIX: EFFECT OF STATIC NET INTERACTION ON EIGENSTATES IN LATTICE OF NONTUNNELING IDENTICAL SQDs

An electron in a dot experiences the electrostatic interaction with the electrons in all other dots as well as with all the positive charges in the system. The interaction with the positive charges depends directly upon the distribution of the donors in the lattice, which makes any calculations of this interaction specific for each distribution. The overall effect of this interaction is some compensation of the effect of the static interdot *e-e* interaction, and the measure of the compensation depends upon the positive charges distribution. In addition depending upon this distribution the lattice of identical SQDs can become a lattice of nonidentical SQDs (in the sense of nonidentical electron eigenstates, interlevel gaps,

etc.) that contributes to inhomogeneous effect on the spectra. In our approach we restrict to the static interdot electron-electron interaction and neglect the interaction with the positive charges. This allows us to avoid bounding to a specific donor distribution. On the other hand, it let us estimate the maximum effect of the static interdot interaction in the lattice.

We assume that the effect of the interdot static *e-e* interaction on the electron eigenstates can be treated as a small perturbation, so that the change of the electron eigenfunctions can be neglected in the first approximation and the correction to the energy levels is

$$E_{\bar{\mathbf{a}}} = E_{\mathbf{a}}^{(0)} + V_{\mathbf{a},\mathbf{a}}^{\mathrm{stat}}, \tag{A1}$$

where $V_{\mathbf{a},\mathbf{a}}^{\mathrm{stat}}$ is the matrix element of the static interdot *e-e* interaction (without the self-interaction) $V^{\mathrm{stat}}(\mathbf{r})$ given by

$$V^{\mathrm{stat}}(\mathbf{r}) = \frac{e^2}{4\pi\epsilon\epsilon_0} \sum_{i,k=-\infty}^{\infty} \int d\mathbf{r}' \frac{1}{|\mathbf{r}-\tilde{\mathbf{r}}'_{ik}|} \sum_{\bar{\mathbf{c}}} |\Phi_{\bar{\mathbf{c}}}(\tilde{\mathbf{r}}'_{ik})|^2 n_{\bar{\mathbf{c}}}. \tag{A2}$$

Developing in the same fashion as in Sec. II A 2 we obtain

$$V_{\mathbf{a},\mathbf{a}}^{\mathrm{stat}} = \sum_{\mathbf{c}} \beta^{\mathrm{stat}}(\mathbf{a},\mathbf{a};\mathbf{c},\mathbf{c}), \tag{A3}$$

where

$$\beta^{\mathrm{stat}}(\mathbf{a},\mathbf{a};\mathbf{c},\mathbf{c}) = \tilde{\beta}^{\mathrm{stat}}(\mathbf{a},\mathbf{a};\mathbf{c},\mathbf{c}) n_{\mathbf{c}} - \beta_{\mathrm{self}}^{\mathrm{stat}}(\mathbf{a},\mathbf{a};\mathbf{c},\mathbf{c}) \tag{A4}$$

and

$$\tilde{\beta}^{\mathrm{stat}}(\mathbf{a},\mathbf{a};\mathbf{c},\mathbf{c}) = \frac{e^2}{2\epsilon\epsilon_0 d_1 d_2} \sum_{\mathbf{G}_{\mathbf{m}_\parallel}} \frac{1}{G_{\mathbf{m}_\parallel}} \int dx_3 dx_3' e^{-G_{\mathbf{m}_\parallel}|x_3 - x_3'|} \times F_{\mathbf{a},\mathbf{a}}(\mathbf{G}_{\mathbf{m}_\parallel}, x_3) F_{\mathbf{c},\mathbf{c}}(\mathbf{G}_{\mathbf{m}_\parallel}, x_3'), \tag{A5}$$

where $\beta_{\mathrm{self}}^{\mathrm{stat}}(\mathbf{a},\mathbf{a};\mathbf{c},\mathbf{c}) = \lim_{d\to\infty} \tilde{\beta}^{\mathrm{stat}}(\mathbf{a},\mathbf{a};\mathbf{c},\mathbf{c})$ is the self-interaction term. Here $F_{\mathbf{c},\mathbf{c}}(\mathbf{G}_{\mathbf{m}_\parallel}, x_3')$ is calculated by Eq. (24), with the upper index "$\pm$" omitted as it is not important. Note, that the form of the relationships for the β for the static interdot *e-e* interaction is the same as for the dynamic *e-e* interaction.

It is seen that $V_{\mathbf{a},\mathbf{a}}^{\mathrm{stat}} > 0$ and, thus, each level moves up in the energy scale. It is Important to note that each level moves up differently, so that the interlevel spacings increase due to the interdot *e-e* static interaction. An interesting feature of Eq. (A3) is that $V_{\mathbf{a},\mathbf{a}}^{\mathrm{stat}}$ is different for different **a** which means that the static interdot interaction splits the states which share the same energy level in a single QD.

One can notice that the effect of the number of the electrons on the modification of the resonant photon energy is different for the dynamic and static interdot *e-e* interactions. The DE shift is proportional to the number of the electrons in the dot [see Eq. (28)]. The shift of each level due to the static interdot *e-e* interaction is also proportional to the number of the electrons in the dot [see Eq. (A4)], however, the interlevel spacing is affected by the electron number only slightly. Figure 8 illustrates the change of the two lowest levels and the gap between them because of the static interdot *e-e* interaction.

*Electronic address: ai8868@wayne.edu

[1] D. Heitmann, V. Gudmundsson, M. Hochgräfe, R. Krahne, and D. Pfannkuche, Physica E (Amsterdam) **14**, 37 (2002), and references therein.

[2] A. I. Yakimov, A. V. Dvurechenskii, N. P. Stepina, and A. I. Nikiforov, Phys. Rev. B **62**, 9939 (2000).

[3] G. Gumbs, D. Huang, H. Qiang, F. H. Pollak, P. D. Wang, C. M. Sotomayor Torres, and M. C. Holland, Phys. Rev. B **50**, 10 962 (1994).

[4] Q. P. Li, K. Karrai, S. K. Yip, S. Das Sarma, and H. D. Drew, Phys. Rev. B **43**, 5151 (1991).

[5] D. A. Broido, K. Kempa, and P. Bakshi, Phys. Rev. B **42**, 11 400 (1990).

[6] L. Wendler and R. Haupt, Phys. Rev. B **52**, 9031 (1995).

[7] M. Taut, Phys. Rev. B **62**, 8126 (2000); **63**, 115319 (2001).

[8] V. Milanovic and Z. Ikonic, Phys. Rev. B **39**, 7982 (1989).

[9] P. A. Sundquist, V. Naryan, J. Vincent, and M. Willander, Physica E (Amsterdam) **15**, 27 (2002).

[10] G. Iadonisi, G. Cantele, V. Marigliano Ramaglia, and D. Nino, Phys. Status Solidi B **237**, 320 (2003).

[11] O. Keller, Phys. Rep. **268**, 85 (1996), and references therein.

[12] H. Ehrenreich and M. Cohen, Phys. Rev. **115**, 786 (1959).

[13] W. M. Que and G. Kirczenow, Phys. Rev. B **38**, 3614 (1988).

[14] W. Que, G. Kirczenow, and E. Castaño, Phys. Rev. B **43**, 14 079 (1991).

[15] V. I. Klimov, D. W. McBranch, C. A. Leatherdale, and M. G. Bawendi, Phys. Rev. B **60**, 13 740 (1999).

[16] M. Shim and P. Guyot-Sionnest, Nature (London) **407**, 981 (2000).

[17] J. Tempere, I. F. Silvera, and J. T. Devreese, Phys. Rev. B **65**, 195418 (2002).

[18] J. Bauer, D. Schuh, E. Uccelli, R. Schulz, A. Kress, F. Hofbauer, J. J. Finley, and G. Abstreiter, Appl. Phys. Lett. **85**, 4750 (2004).

[19] E. L. Ivchenko and A. V. Kavokin, Sov. Phys. Solid State **34**, 1815 (1992).

[20] V. Bondarenko and M. Załużny, J. Phys.: Condens. Matter **12**, 8267 (2000).

[21] A. Vasanelli, M. De Giorgi, R. Ferreira, R. Cingolani, and G. Bastard, Physica E (Amsterdam) **11**, 41 (2001).

[22] G. Ya. Slepyan, S. A. Maksimenko, V. P. Kalosha, A. Hoffmann, and D. Bimberg, Phys. Rev. B **64**, 125326 (2001).

[23] M. Załużny and C. Nalewajko, Phys. Rev. B **59**, 13 043 (1999).

[24] P. Bakshi, D. A. Broido, and K. Kempa, Phys. Rev. B **42**, 7416 (1990).

[25] R. K. Pandey, Manoj K. Harbola, and Vijay A. Singh, Phys. Rev. B **67**, 075315 (2003).

[26] V. Bondarenko and Y. Zhao, J. Phys.: Condens. Matter **15**, 1377 (2003).

[27] G. Todorovic, V. Milanovic, Z. Ikonic, and D. Indjin, Phys. Rev. B **55**, 15 681 (1997).
[28] M. Załużny, Phys. Status Solidi B **123**, K57 (1984); **161**, K19 (1990).
[29] D. P. Dave and H. F. Taylor, Phys. Lett. A **184**, 301 (1994).
[30] W. M. Que and G. Kirczenow, Phys. Rev. B **39**, 5998 (1989).
[31] A. Bagchi, R. G. Barrera, and R. Fuchs, Phys. Rev. B **25**, 7086 (1982).